Chapter -2

Literature Review

2.0 Introduction

This chapter presents current literature reviewed to underpin the empirical part of this research work. The main contents in this chapter include information about the different welding processes used in industries, different steels, weld metallurgy, quality in welding, productivity in welding, and economy in welding. Much emphasis is laid on welding process, microstructure and types of steels.

An attempt has been made through this chapter to scientifically present some of the significant studies towards the understanding of the above-mentioned topics and methods to improve the weld quality during fusion welding of IS2062 steel and AISI 304 steel under different welding conditions. Many investigations have been carried out on the various aspects of Gas Metal Arc (GMA) welding; the following aspects have been selected for literature review:

1. Review of welding
2. Different welding process
3. Effect of welding process parameters on IS 2062 structural steel welded joint
4. Effect of welding parameters on SS304 welded joint
5. Effect of welding parameters on various metals
6. Study of process modeling, simulation and their application in gas metal arc welding(GMAW)

2.1 Review of Welding

2.1.1 Middle Ages

Welding can trace its historic development back to ancient times. The earliest examples come from the Bronze Age. Small gold circular boxes were made by pressure welding lap joints together. It is estimated that these boxes were made more than 2000 years ago. During the Iron Age, the Egyptians, and people in the eastern Mediterranean area learned to weld pieces of iron together. Many tools were found which were made approximately 1000 B.C.

During the Middle Ages, the art of blacksmithing was developed and many items of iron were produced which were welded by hammering. It was not until the 19^{th} century that welding, as we know it today was invented.

2.1.2 from 1800 to 1900

Edmund Davy of England is credited with the discovery of acetylene in 1836. The production of an arc between two carbon electrodes using a battery is generated by Sir **Humphry Davy** in 1800 and approximately 1900 century; Strohmenger discovered a coated metal electrode in Great Britain. There was a thin coating of clay or lime, but it provided a great stable arc. Oscar Kjellberg of Sweden discovered a covered or coated electrode from a period of 1907 to 1914.

2.1.3 from 1902 to most recent

In 1920, automatic welding was introduced. It utilized bare electrode wire, operated on direct current and utilized arc voltage as the basis of regulating the feed rate. Gas tungsten arc welding (GTAW) had its beginnings from an idea by C.L. Coffin to weld in a non-oxidizing gas atmosphere, which he patented in 1890. The concept was further refined in the late 1920s by H.M.Hobart, who used helium for shielding, and P.K. Devers, who used argon. In 1953, Lyubavskii and Novoshilov announced the use of welding with consumable electrodes in an atmosphere of CO_2 gas and today the science continues to advance. Friction stir welding, Electron beam welding, Laser beam welding, underwater welding, Robot welding is becoming a more commonplace in industrial settings, and researchers continue to develop new welding methods and gain a greater understanding of weld quality and properties. Friction welding, which uses rotational speed and upset pressure to provide friction heat, was developed in the Soviet Union [5].

2.2 Welding process

2.2.1 Arc welding

Today several electric arc welding process are very commonly used in industry. In electric arc welding process, heat is produced between a copper coated electrode and workpiece [6].In electric arc welding process a high degree of temperature from 3500°C-5500°C is produced, which is sufficient to melt the base metal and filler wire. The basic function of filler/electrode is to fill the groove. Electric arc welding is of different types such as manual metal arc welding (MMAW) or shielded metal arc welding (SMAW), Gas Tungsten arc welding (GTAW), Gas metal arc welding (GMAW), Flux cored arc welding (FCAW), Submerged arc welding (SAW) and many more. Depending on the welding work to be carried out, each welding process having some special characteristics. Among the various electric arc welding, Gas Metal Arc welding (GMAW) is very common and frequently used in industries for mass production to weld the ferrous and non-ferrous materials [6].

2.2.2 Manual metal arc welding

Manual metal arc welding or shielded metal arc welding is frequently used in construction, fabrication and repair industries. MMA welding consists of creating a high-intensity electric arc between a shielded metal-cored electrode and the metals to be joined. The filler metal is transferred by an electric arc between the gushing soul of the coated electrode and the base plate.

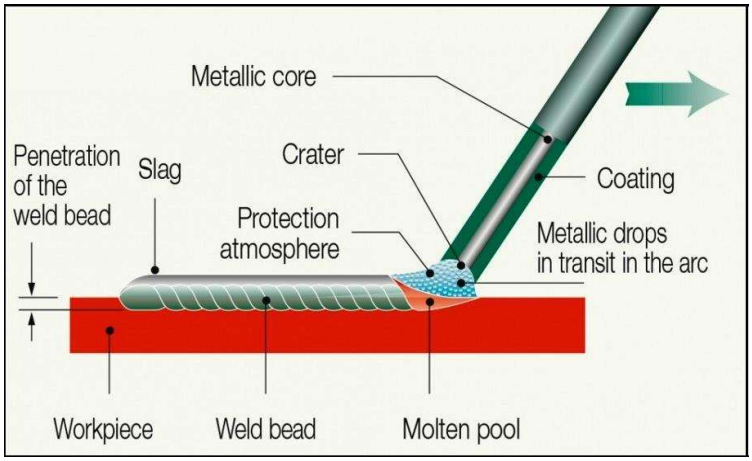

Figure 2.1 Working principle of MMA welding [7]

Heat generated by the electric arc simultaneously melts the base plate (workpiece), the metal core and the coating of the electrode, creating the melt which collects drops of filler metal and molten slag transferred into the plasma of this arc.

2.2.3 Gas Metal Arc Welding (GMAW)

2.2.3.1 Principle of GMAW process

Gas metal arc welding was developed in 1950 and it is also known as Metal Inert Gas (MIG) welding [8] or metal active gas welding process, in which an electric arc is produced between a consumable copper coated electrode and base metal, which heats the object, causing them to melt and bond. For shielding purpose, an inert gas or gas mixture is used, which protect molten metal from any contamination. GMA welding is extensively used in metal fabrication industries [8] as all commercial important metals like carbon steel, stainless steel, copper, and aluminum can be easily weld for all position, GMA welding can be easily mechanized [9].Working principle of GMA welding process is shown in the figure in 2.2

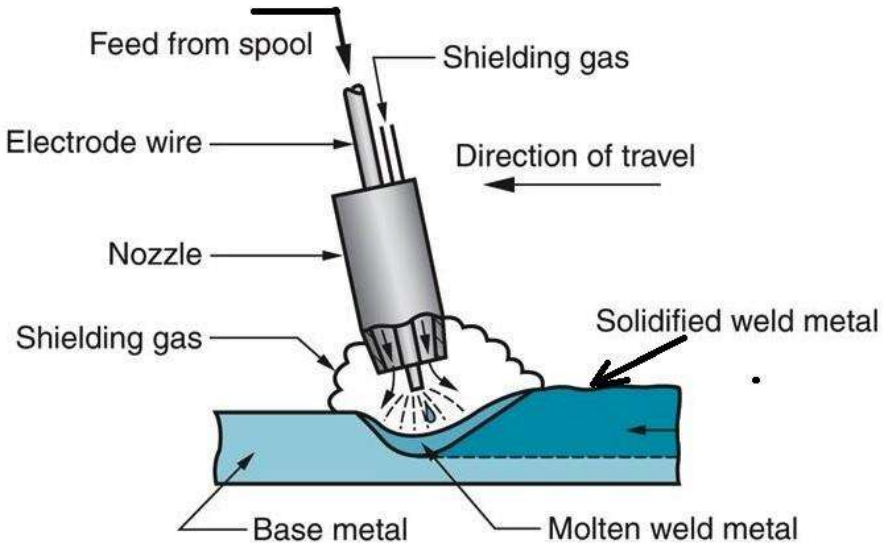

Figure 2.2: Schematic of GMAW process [8]

The essential elements of a basic GMAW process are shown in Figure 2.3.GMAW is an arc welding process that incorporates the automatic feeding of a continuous, copper coated electrode

that is shielded by an externally inert gas (Figure 2.4) to avoid any contamination of molten metal from the atmosphere.

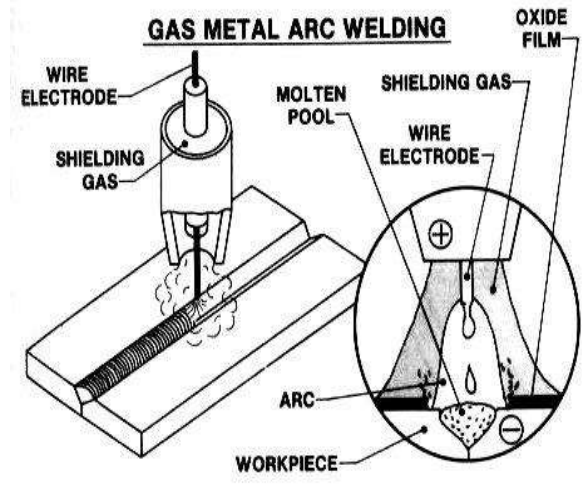

Figure 2.3 The essential elements of a basic GMAW process[10]

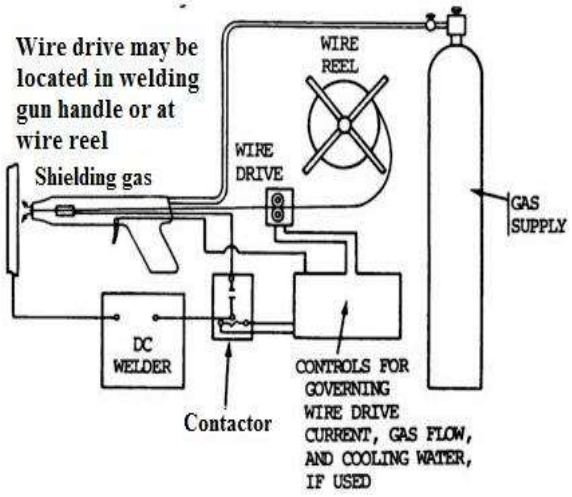

Figure 2.4 GMAW incorporates the automatic feeding of a continuous, consumable electrode that is shielded by an externally supplied gas [11]

2.2.3.2 Advantages of GMAW process

- GMA Welding can be formed in all positions.
- GMA welding provides deeper penetration than MMA welding process is possible, which in some circumstances permit the use of smaller-sizes fillet for equivalent strength.
- GMA welding speed is faster than those of the MMA welding process.
- GMA welding process can be easily mechanized.
- The deposition rate is significantly higher than those obtained by the MMA welding process.
- X-ray quality weld can be produced.
- GMA welding process provides the high quality of mechanical properties and microstructure of weldment.

- Skill operator is not required in GMA welding process as compared to any other welding process.

2.2.3.3 GMA Welding Process parameters

The following are some important welding parameters that affect the mechanical properties and microstructure of (IS 2062 and AISI 304 steels) weldments.

(1) Welding current

(2) Arc voltage

(3) Arc travel speed

(4) Wire feed speed

(5) Heat input

(6) Shielding gas flow rate

(7) Metal transfer mechanism

(8) Electrode diameter

(9) Polarity

The parameters varied were the welding current, wire feed speed, and shielding gas flow rate. Effect of these variables on Gas Metal Arc (GMA) Welding process and weldability are briefly described below [10]

2.2.3.3.1 Welding current

According to equation 2.1, heat input and welding current are directly related; on increasing the weld current, heat input increases. It is used to determine the melting rate of the electrode, the amount of base metal melted, dilution, and the weld bead geometry. On increasing the welding current, amount of filler wire increases and weld reinforcement. Figure 2.5 shows the effect of welding current on weld bead profile.

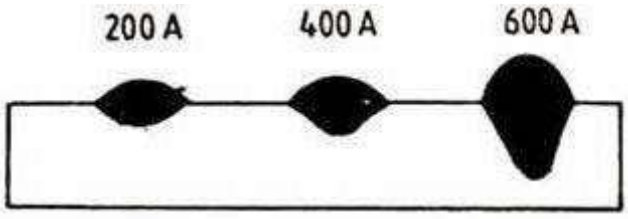

Figure 2.5 Effect of welding current on weld bead geometry [14]

Asibeluo I.S, Emifoniye E. (2015) welded A36 carbon steel with shielded metal arc welding process by considering the welding current range from 70A-120A for welding purpose and they concluded that on increasing the welding current from 70-120A increase the welding heat input, which affects the microstructure of the weld itself and provides impact to the strength and hardness of the weldment. The increase in welding current results in increases in temperature of the weld and results in the depletion of toughness and hardness as a result of increased cooling time which gives rise to the rapid growth of the grain [11].

2.2.3.3.2 Arc voltage

An electric arc is the form of electric discharge with the highest current density. The maximum current through an arc is limited only by the external circuit, not by the arc itself [12]. Arc voltage affects the weld bead shape and the depth of penetration, the precise effect being dependent on the joint preparation. Bead on plate welds and square edge close butt welds have increased weld bead width and dilution as the arc voltage increases, although the depth of penetration is relatively unaffected. In a prepared V-butt joint, increasing the arc voltage may lead to lack of fusion in the root as the wide arc will not reach the bottom of the root. Decreasing in arc voltage, increase the depth of penetration as the narrow arc column is able to reach the bottom of the weld preparation [13]. Figure 2.6 shows the effect of arc voltage on weld bead shape and its size.

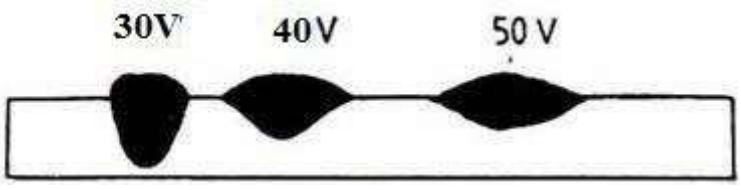

Figure 2.6 Effect of arc voltage on weld bead shape and its size [14]

Shapes of the weld bead cross section principally determined by arc voltage and its external appearance. As on increasing the welding voltage with constant current and constant welding speed produces wider, flatter, less penetrated weld beads and tends to reduce the porosity produced by rust or scale on steel. Higher voltage is responsible an excessive root opening when fit-up is not uniform. Increase in arc voltage also increases the size of droplets and hence decreases the number of droplets and the time of the movement of droplet transfer also increase. Further increase in arc voltage, increases the possibility of breaking the arc and disrupting the normal welding process. Therefore increase in voltage also affects the mechanical and metallurgical properties of the weldment {Izzatul Aini Ibrahim et al 2012(15), S. Ragu Nathan et al 2010(16)}.

Talabi, S.I.et al (2014) studied the effect of various welding parameters on mechanical properties of low carbon steel welded joint and the authors mentioned in their result that selected welding parameters had a significant effect on mechanical properties and microstructure on weldment. On increasing in arc voltage and welding current, increases in hardness and decreases in yield strength, UTS, and toughness [17].

2.2.3.3.3 Arc travel speed

Arc travel speed influences the mechanical properties as well as the microstructure of weldment as it is a function of a heat input. The width of weld bead and penetration is controlled by welding speed [18-19].On increasing the welding speed, heat input/unit length decreases, as welding speed is inversely proportional to heat input, less filler wire is used/unit length of the weld, resulting in less weld reinforcement. Figure 2.7 shows the effect of different welding speeds on weld bead width and its profile.

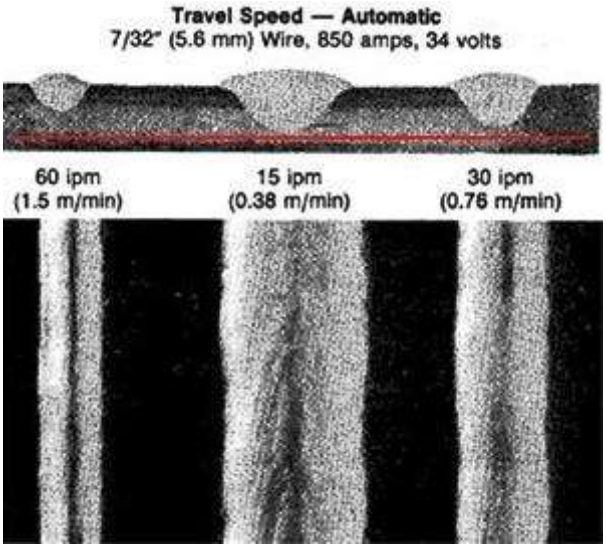

Figure 2.7 Effect of welding speeds on weld bead width and its profile [20]

Amount of porosity in a weldment is also influenced by welding speed. Higher welding speed increases penetration, thus resulting in increasing the dilution in weld [21]. If the welding speed decreases within a certain point, the penetration also decreases, it is only due to the pressure of the large amount of weld pool beneath the electrode, which will reduce the arc penetrating force [22].Excessive welding speed resulting in the undercut, arc blow problem, cracking, uneven bead geometry, and also increases the slag inclusion in the weldment. Higher welding speed results in fine grain size and less HAZ. While a relatively very low welding speed promotes coarse grain in microstructure [23].

H.R. Ghazvinloo et al (2010) considered arc voltage, welding current, and welding speed as welding parameters during the welding of AA6061 and they concluded that when heat input increases, fatigue life of welded joint decreases whereas impact energy (Toughness) of welded joint increases first and then drops significantly [24].

Shekhar Srivastava and R.K Garg, (2017) considered Welding parameters such as welding speed, wire feed speed, and arc voltage during the welding of IS2062 steel and they optimized the welding parameters by applied Taguchi technique and through ANOVA they predict significance of process parameters, wire feed rate followed by arc voltage and travel speed has been found as

the sequence of effective parameter among all uses in this study. The gas flow rate was least effective parameter [25].

2.2.3.3.4 Wire feed speed

Wire feed speed is also another important parameter which influences the weld bead as well as mechanical properties of a weldment. Wire feed speed is expressed in meter per minute (m/min).The wire feed speed serves another purpose for regulating the amperage. When stick or GTA welding, the basic setting is amperage, but it is the arc voltage that fluctuates depending on the length of an arc. The tensile strength and microhardness of weldment increased when arc current, welding voltage increased, and travel speed decreased [26]. Figure 2.8 shows the graph between welding current and wire feed speed for different diameters of carbon steel filler wire.

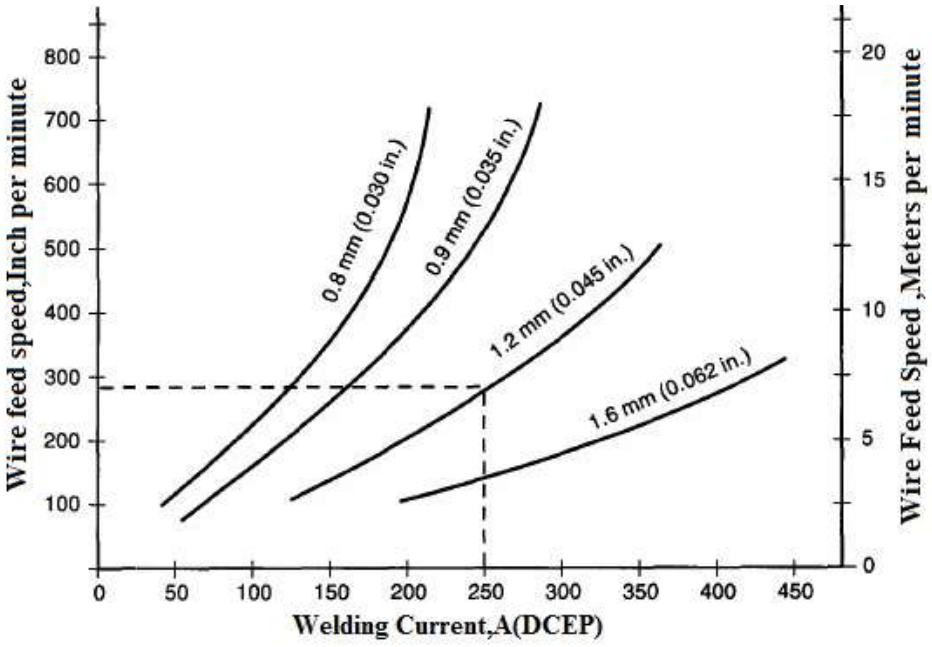

Figure 2.8 Welding current Vs wire feed speed for various diameters of carbon steel [27]

Table 2.1 shows the material thickness and recommended wire feed speed with gas flow rate.

Table 2.1 Manual travel, single pass, and flat fillet welds [28]

(Manual travel, single pass, flat fillet welds)

S.No.	Material Thickness(inches)	Electrode size	Welding DCRO (Arc Volts)	Conditions (A)	Gas flow rate(cfh)	Travel speed(ipm)
1	0.025	0.030	15-17	30-50	15-20	15-20
2	0.031	0.030	15-17	40-60	15-20	18-22
3	0.037	0.035	15-17	65-85	15-20	35-40
4	0.050	0.035	17-19	80-100	15-20	35-40
5	0.062	0.035	17-19	90-110	20-25	30-35
6	0.078	0.035	18-20	110-130	20-25	25-30
7	0.125	0.035	19-21	140-160	20-25	20-25
8	0.125	0.045	20-23	180-200	20-25	27-32
9	0.187	0.035	19-21	140-160	20-25	14-19
10	0.187	0.045	20-23	180-200	20-25	18-22
11	0.250	0.035	19-21	140-160	20-25	10-15
12	0.250	0.045	20.23	180-200	20-25	12-18

2.2.3.3.5 Heat input

Heat input is also another important welding parameters which influence the mechanical properties and microstructure of a weldment. A literature review of weldment cannot be overlooked without discussion of heat input. Heat input is a relative measure of the energy transferred per unit length of a weldment. It is an important characteristic as it also influences the metallurgical structure of weldment. Heat input is calculated by the given formula [29]:

$$\text{H.I}=\frac{(VxIx60)}{(Sx1000)}\,x\eta \text{ ---------(2.1)}$$

Where H.I=heat input (kJ/mm), V=arc voltage (V), I=welding current (A), S=arc travel speed (mm/s), and η=arc efficiency.

For Gas metal arc welding (GMAW) η=0.9

Ehsan Gharibshahiyan et al (2011) welded low carbon steel with GMA welding and they concluded from their result that at high heat input, coarse grains appear in the HAZ which results in lower hardness values in this zone. High heat input and low cooling rates produced fine austenite grains, resulting in the formation of fine-grained polygonal ferrites at ambient temperature [30].

T.A.Tabish et al (2014) considered SS304 material for their research work and they found from their result that the weldment was stronger than the base metal and strength varies across the joint. Low heat input produced fine structured fusion and the microstructural study reveals that high heat input produced larger dendrites than those produced with a medium, and low heat input [31]. Figure 2.9 shows the microstructure of weldment at different heat input.

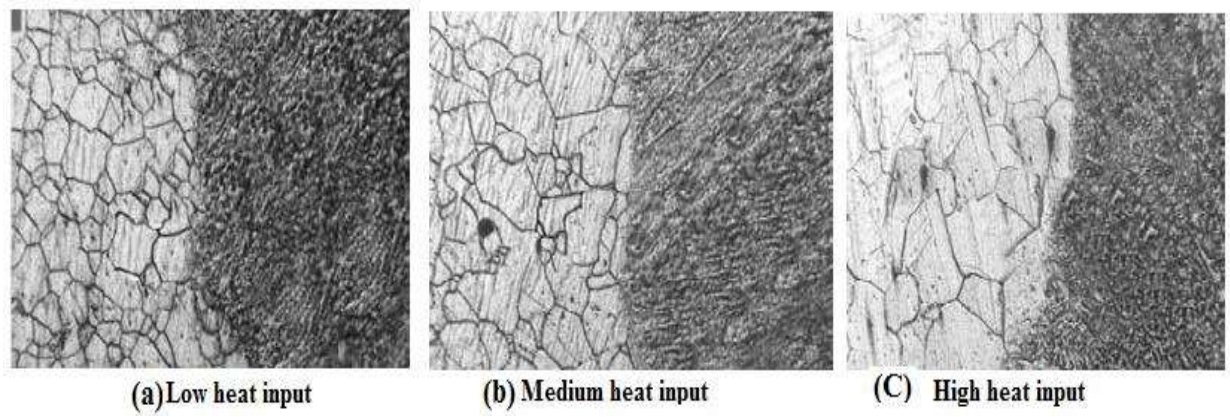

Figure 2.9 shows the microstructure of weldment at different heat input [31]

Wan Shaiful Hasrizam Wan Muda et al (2015) determined the effect of heat input on microstructure and mechanical properties at HAZ of ABS grade steel and they reported in their result that microstructure formation at CGHAZ was consisting of grain boundary ferrite (GBF), Widmanstatten ferrite (WF) and pearlite (P). Significant grain coarsening was observed at the CGHAZ of all the joints, and it was also found that the extent of grain coarsening at CGHAZ has also increased along with the heat input. Figure 2.10 shows the micrograph of weldment at different heat input.

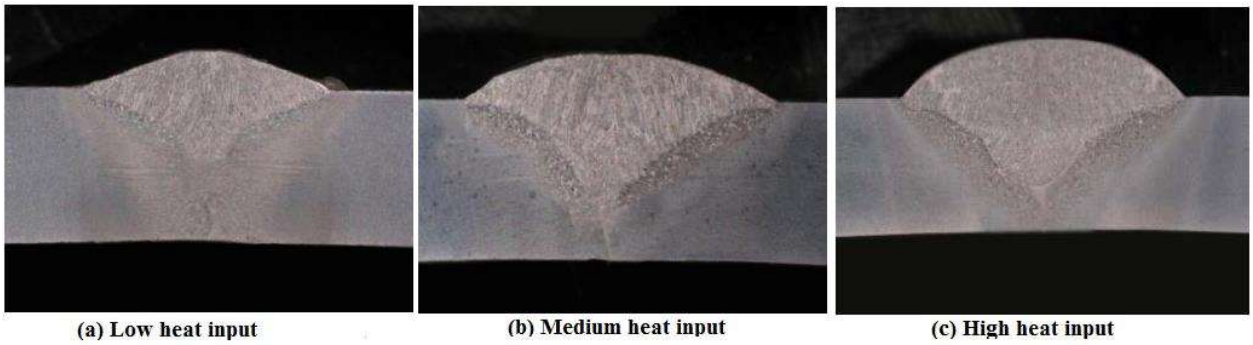

Figure 2.10 shows the micrograph of weldment at different heat input [32]

Subodh Kumar and A.S. Shahi, (2011) studied the effect of heat input on mechanical properties and microstructure of AISI 304 welded joints by GTA welding and they concluded that joints fabricated at low heat input exhibited higher ultimate tensile strength (UTS) than those welded with medium and high heat input respectively. Significant grain coarsening was observed in the heat affected zone (HAZ) of all the welded joints and extent of grain coarsening in the heat affected zone increased with increase in the heat input. It was also found that average dendrite length and inter-dendritic spacing in the weld zone increases with increase in the heat input which is results in changing in the tensile properties of the weld joints, welded with different arc energy inputs. Figure 2.11 shows the microstructure of weldment and fusion zone at different heat input.

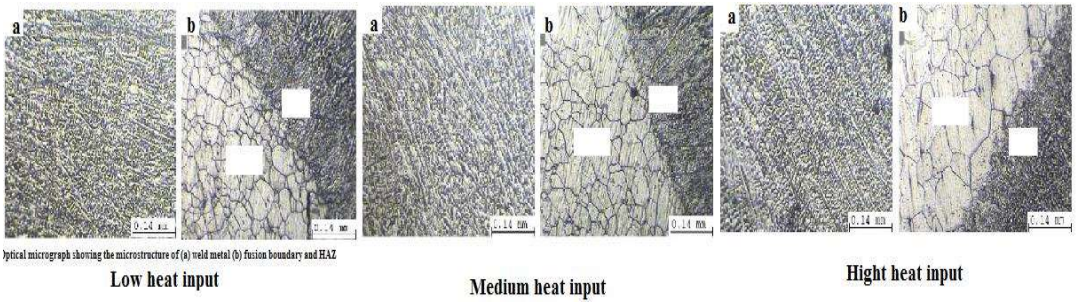

Figure 2.11 Optical micrograph showing the microstructure of (a) weld metal, (b) fusion boundary, and HAZ at low, medium and high heat input [33]

2.2.3.3.6 Shielding gas flow rate

Shielding gas flow rate, too much influence the microstructure and the weld bead profile of a weldment. Different shielding gases and their mixtures are used for shielding purpose. One of the

major functions of shielding gases is to prevent atmospheric contamination of the weldment. Figure 2.12 shows the effect of different shielding gases on weld bead profile and penetration. In general Ar, He, CO_2, O_2, N_2 and their mixture in various proportions are used for shielding purpose. Argon is used in welding of carbon steel, stainless steel, and low thickness plate of aluminum alloys. 5% of H_2 gas is mixed with argon for frequently joining of Austenitic stainless steels as H_2 increases arc-voltage and consequently heat input, increasing penetration of welded joint and support to improving the weld bead appearance[34].

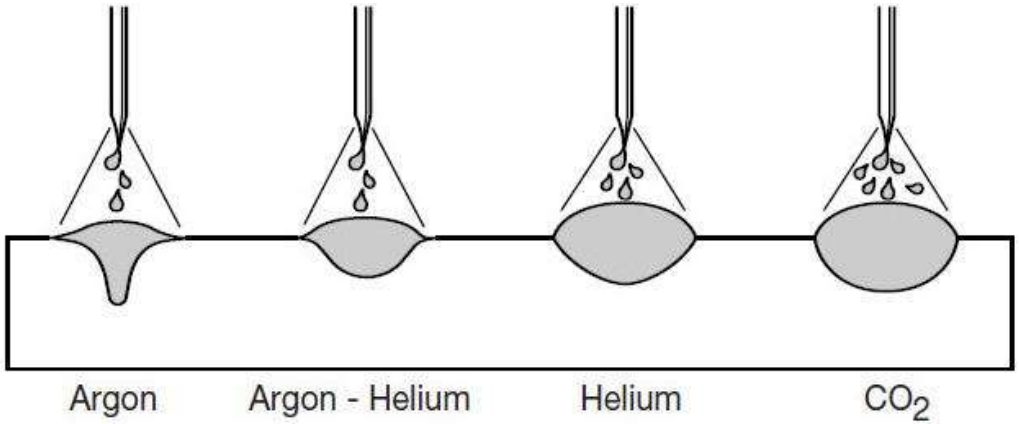

Figure 2.12 Effect of different shielding gases on weld bead profile and penetration [35]

S. Mukhopadhyay and T.K. Pal, (2006) performed welding on HSLA steel with GMA Welding under different shielding gas mixture Ar, CO_2 and O_2 and from their result they observed that microstructures of HSLA weldment (constituents such as AF, GF, and Ferrite with Side plate FS in HSLA weld metals) are influenced by the oxygen and carbon dioxide content in the shielding gas [36]. The optical microstructures obtained in the weld metal for both solid and flux-cored wires by using mixture of different shielding gas is shown in Fig. 2.13.Figure 2.13 a to d shows the microstructure of an HSLA steel weldment under different shielding gases environment. Figure 2.13 a shows the formation of ferrite and pearlite while figure 2.13 b & c shows the formation of polygonal ferrite & widmanstatten ferrite. Process condition of different morphology is listed in Table No.2.2

Table 2.2 Process condition of different morphology

Sample No.	Gas composition ($Ar-CO_2-O_2$)	Current (A)	Voltage (V)	Speed (Cm/min)
S1	80-18-2	214	32	28
S4	80-15-5	214	32	28
F1	80-18-2	234	32	27

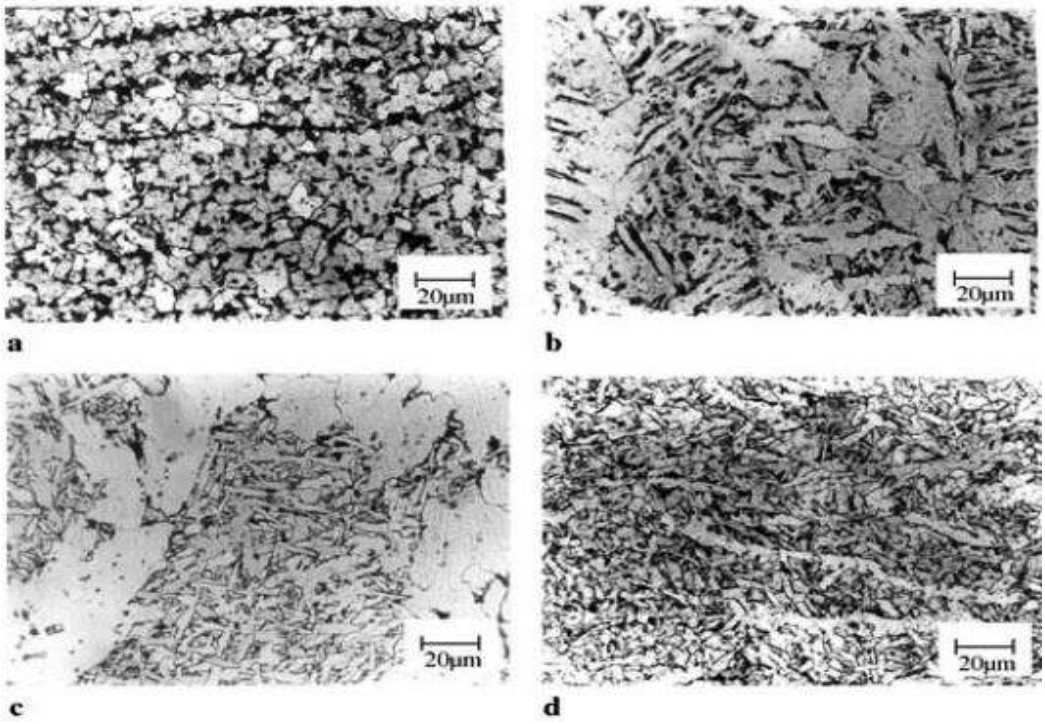

Figure 2.13 a-d. Microstructure of (a) base plate (b) weldment sample S1,(c) sample S4 (d) sample F1[36]

P. Sathiya et al, (2009) welded Duplex stainless steel 2205 with TIG welding under the envelope of Shielding gases (Ar & He) and they indicated in their result that hardness of the weld metal is much higher than that of the BM and HAZ for both shielding gases [2.44]. Different shielding gases and their mixture having different properties for a specific material. Table 2.3 shows the different shielding gases and their properties for a weldment.

Table 2.3 Shielding gases and their properties for a weldment.

S.No	CO_2	$Ar+CO_2$	$Ar+O_2$
1	Higher fume levels	Lower fume levels	Lowest fume levels
2	Deeper penetration	Shallow penetration	More rounded penetration
3	More violent or inconsistent arc transfer	Smoother arc transfer	Smoother arc transfer
4	Lower cost	Higher cost	Higher cost
5	Higher spatter	Lower spatter	Lowest spatter
6	Less radiated heat	More radiated heat	Most radiated heat
7	Less attractive beads	More attractive beads	attractive beads
8	Pulse welding not possible	Pulse welding possible	Pulse welding possible
9	Metal transfer in the form of spray not possible	Metal transfer in the form of spray possible	Metal transfer in the form of spray possible

E. Taban et al (2014) considered AISI 304 austenitic stainless steel and welded by GTAW with using different Shielding-gas such as Pure Ar, N_2,H_2 in different proportions and it was found from result that various purging gases affect corrosion properties as well as the amount of the heat that occurred at the roots of the welds. Mechanical properties were not considerably affected due to purging gases [37].

Behçet Gülenç et al (2005) studied the effect of hydrogen in argon as a shielding gas in GMA welding of ASS and authors concluded that Increasing hydrogen content in argon as a shielding

medium increased the penetration profile, depth, and width of weld bead [38]. Figure 2.14 shows the microstructure of SS 304 under different shielding and current range.

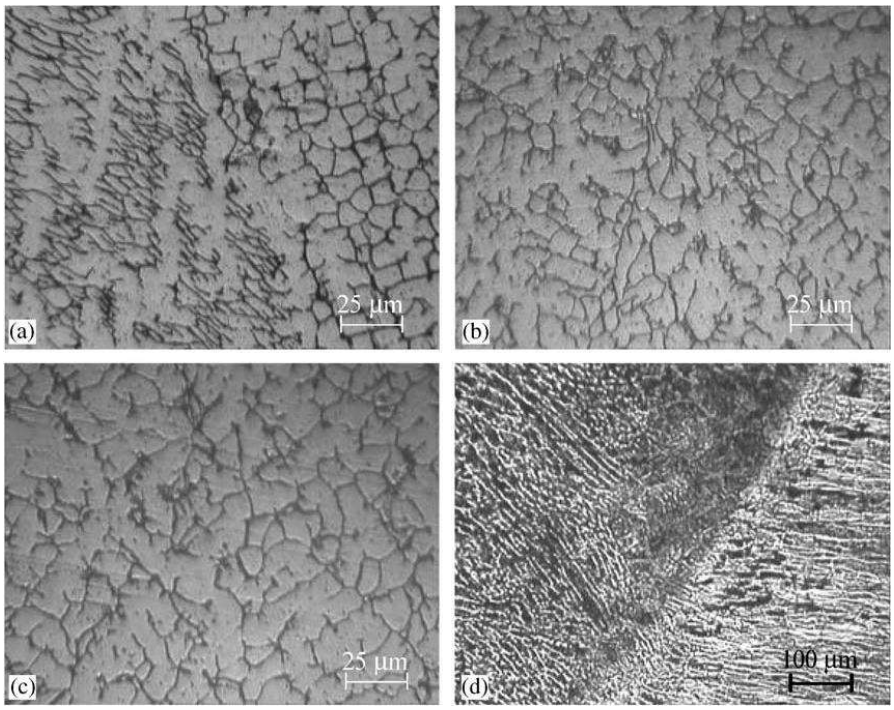

Figure 2.14 Optical microstructures of the samples welded under the shielding of 1.5% H_2–Ar with different welding current: weld metal structure welded with (a) 140A, (b) 180A, (c) 240A and (d) transition zone structure welded with 140A [38].

Mohamad Ebrahimnian et al, (2009) studied the influence of variation in the shielding gas composition on the weld properties of the ST 37-2 steel. They considered the two shielding gases i,e Ar and CO_2 mixture in four compositions and from their results they found that on increasing the amount of CO_2 in shielding gas, leads to reducing the amount of inclusion and porosity, and volume fraction of acicular ferrite reduced, and volume fraction of widmanstatten ferrite increase with increasing of the CO_2 amount in shielding gas [39]. Figure 2.15 shows the microstructure of ST 37-2 steel weldment with 82%Ar+18%CO_2 shielding gas mixture having Acicular ferrite (AF),widmanstatten ferrite(WF) and polygonal ferrite (PF).

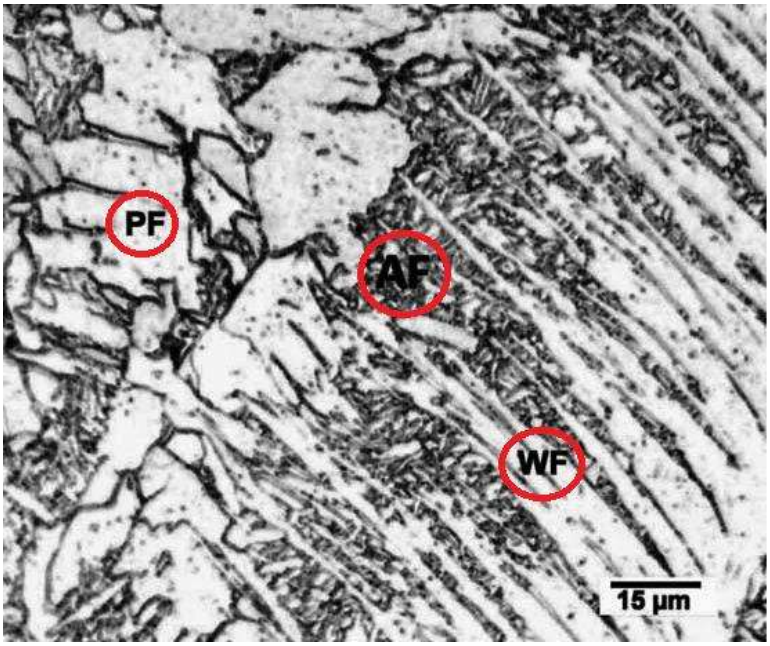

Figure 2.15 Metallographic micrograph of ST 37-2 (82% Ar + 18% CO_2) weld pool etched in 2% Nital, AF: acicular ferrite, WF: Widmanstatten ferrite, PF: polygonal ferrite [39]

2.2.3.3.7 Metal Transfer in GMAW Process

The metal transfer has been a subject matter of many investigations. In the welding process, the metal transfer was controlled and its mode was detected by monitoring current and voltage of the power supply [40]. Most of the recent investigations focused on studying the effect of waveform parameters on the mode of metal transfer in pulsed gas metal arc welding (GMAW-P) [41-43]. The metal transfer mode is also an interesting subject, matter in newly developed welding methods such as double electrode gas metal arc welding (DE-GMAW) developed at the University of Kentucky [44].

Metal transfer in GMAW recognized as a process of transferring material of the welding wire in the form of molten liquid droplets to the work-piece (Figure 2.16). Metal transfer plays an important role in determining the process stability and weld quality. Depending on the welding conditions, the metal transfer can take place in three principal modes: globular, spray, and short-circuiting. Globular transfer, where the droplet diameter is larger than the wire diameter, occurs at relatively low currents. Since it is often accompanied by extensive spatters, a globular transfer is

typically used in welding parts which have relatively loose quality requirements. Spray transfer, where the droplet diameter is smaller than the wire diameter, occurs at medium and high currents. It is a highly stable and efficient process and is widely used in welding thick steel plates, and aluminum parts. The short-circuiting transfer is a special transfer mode where the molten droplet on the wire tip makes direct contact with the workpiece or the surface of the weld pool. It is characterized by repeated, intermittent arc extinguishment and re-ignition. It requires low heat input and hence is commonly used in welding thin sheets. Figure 2.16 shows the various mode of metal transfer in GMA welding process.

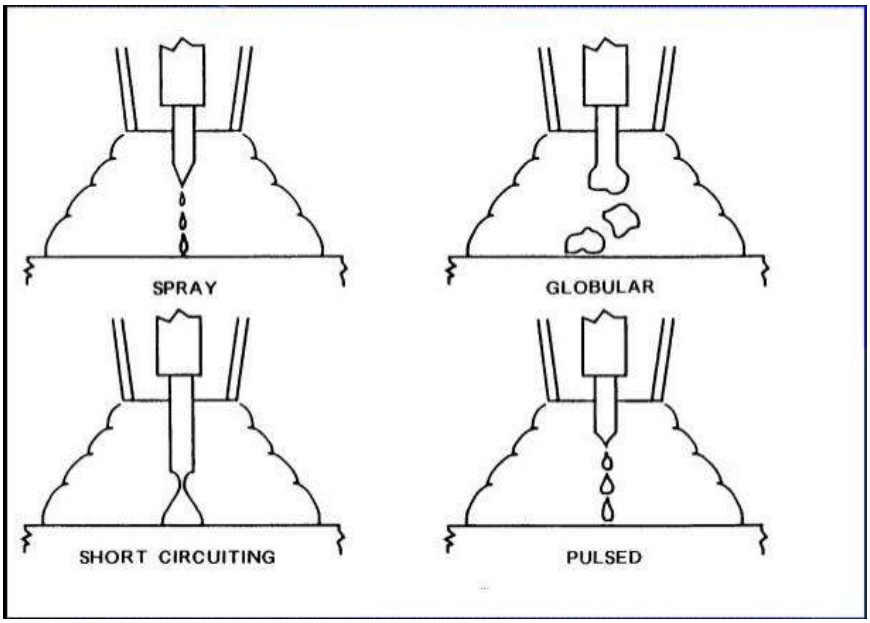

Fig. 2.16 Schematic of metal transfer process in GMAW [45]

Among the Stainless steel welding processes, automated GMAW-P has been recognized as an efficient alternative for minimizing defects [46-48]. In GMAW-P, droplets are regularly detached at a fixed frequency and directionally transferred to the workpiece under influence of current waveform.

As one of the widely used aluminum welding methods, the GMAW process needs improvements in order to achieve higher weld quality and higher productivity. Since the characteristic of metal transfer in GMAW significantly affects the weld quality especially with respect to its microstructure, porosity formation, strength, and fatigue properties etc.

2.2.3.3.8 Electrode diameter

Electrode diameter is also another major welding parameter. It affects the weld bead geometry at constant current. In GMA welding process a continues copper coated wire is used. On increasing the diameter of the electrode, increases in heat input and also promotes longer weldment cooling time. Electrode diameter also influences the metal deposition rate [49]. For welding of thin materials, the electrode diameter should lie from 0.23" to 0.035". For medium thick sheet, electrode diameter should be 0.045" and for a heavy plate, it should be 1/8". Figure 2.17 depicts the effect of electrode diameter size on the amount of reaustenitised and tempered weld metal in multipass welding, white areas represent reaustenitised and tempered weld metal.

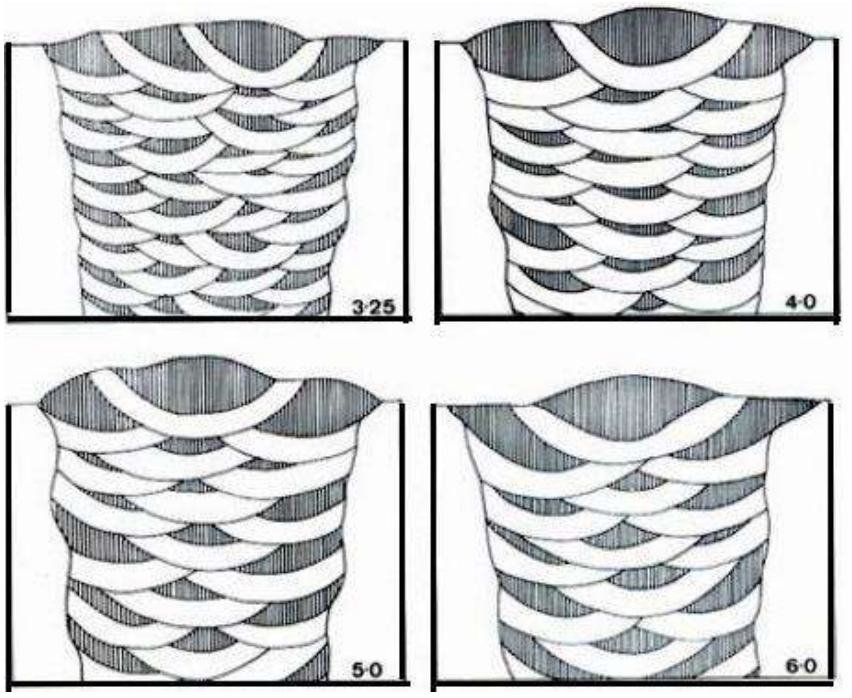

Figure 2.17 Effect of electrode size on an amount of reaustenitised and tempered weld metal in multi-run welding, cross sections as a function of weld diameter, white areas represent reaustenitised and tempered weld metal. The electrode diameters are mention in the bottom right-hand corner of each figure. [49]

2.3 Heat Transfer to the base metal in GMAW

Calorimeter-based heat-transfer experiments reveal that the heat-transfer efficiency for welding thick-section steel is nominally 80 to 90%, as indicated in Figure 2.18. The total heat-transfer efficiency is altered somewhat by changing other parameters. For example, it increases slightly as the power supply open-circuit voltage is decreased for a silicon controlled rectifier regulated power supply and it increases slightly with increasing contact tube-to-base metal distance. However, 85% is a reasonable estimate for most conditions.

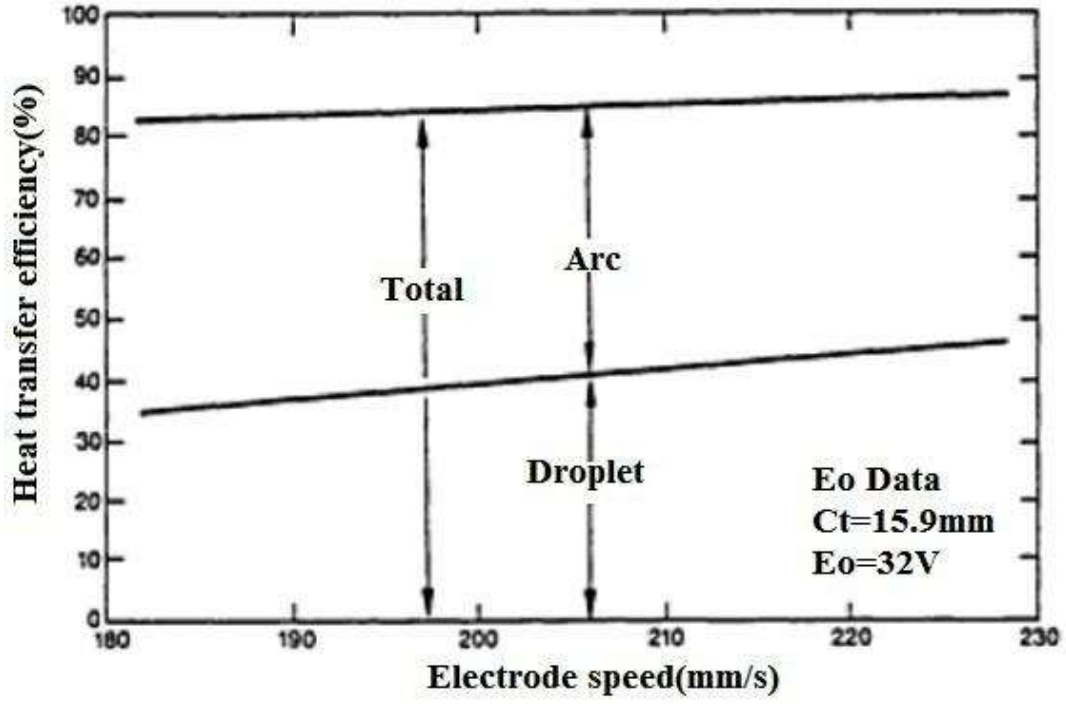

Fig. 2.18 Plot of Heat-Transfer Efficiency to Base Metal V_s Electrode-Speed [22]

In the GMAW process, the molten droplets of electrode material carry a significant portion of the total heat transferred to the weld pool. This is seen in calorimetry experiments, where the total heat transfer efficiency of the GMAW process is partitioned into those portions associated with transfer by the arc and by the molten droplets. At low electrode speeds, about 60% of the total heat transferred is associated with the arc. As electrode speed increases, the fraction of total heat transferred associated with the droplets increases, reaching nominally 50% at current levels in excess of about 220 A for the conditions used.

2.4 Weldability of steels

In general, weldability is also known as joinability and defined as the ability to weld the material under the different welding conditions. The good weldability is ensured by placing a maximum allowable value on HAZ hardness which is controlled by keeping the carbon equivalent (CE) lower critical level. Microstructure, hardness, and toughness of a HAZ are the three major parameters that are used to quantify the weldability of steel.

Some common feature of weldability:-

- Weldability is the capacity of a material to be welded under a specific set of fabrication and design conditions and to perform as expected during its service life
- Weldability is considered very good for low-carbon steel (carbon level, < 0.15% by weight), good for mild steel (carbon level, 0.15 to 0.20%), fair for medium-carbon steel (carbon level, 0.20 to 0.50%), and questionable for high-carbon steel (carbon level, 0.50 to 1.00%)
- Weldability normally decreases with increasing carbon content. In addition to carbon content, the presence of other alloying elements will have an effect on weldability
- A quantitative approach to determine the weldability of steel is to calculate its *carbon equivalent value*.
- The combined effect of carbon and other alloying elements on the weldability is given by "carbon equivalent value (C_{eq})" which is given by the following formula [50-51] as per International Institute of Welding(IIW):-

$$CE = \%C + \frac{\%Mn}{6} + \frac{(\%Cr + \%Mo + \%V)}{5} + \frac{(\%Cu + \%Ni)}{15} \quad \text{——(2.2)}$$

- CE = Carbon Equivalent
- C = Carbon
- Mn = Manganese
- Ni = Nickel

- Cr = Chromium
- Mo = Molybdenum
- V = Vanadium

The steel is considered to be weldable without preheating if C_{eq} < 0.42%. However, if carbon is less than 0.12% then C_{eq} can be tolerated up to 0.45%.

2.4.1 Metallurgical factors affecting weldability

Following metallurgical factors influence the weldability of a material:-

2.4.1.1 Hardenability

In steel, hardenability is generally used to indicate austenite stability with alloying element additions. It is also used to indicate the weldability and as a guide for selecting a raw material and appropriate welding process to avoid any cracking and excessive hardness in the HAZ of a weldment. Steel with high hardness often contains a high volume fraction of martensite, which is responsible for cracking during welding. It is also used to determine hydrogen induced cracking. Carbon equivalent (CE) is an expression; which is used to estimate the cracking susceptibility of steel during welding, and use to determine whether the steel needs pre- and post-weld heat treatment to avoid cracking.

2.4.1.2 Weld metal and HAZ properties

2.4.1.2.1 Weld metal

The weld metal is a fusion zone, in which the copper coated filler wire melts in between the groove and solidified, and bonds with the base plate. A shielding gas or gas mixture is used to avoid any contamination of molten metal pool from the atmosphere. Figure 2.19 shows the interaction between the heat source and various zones of a weldment. i.e. base metal (Unaffected zone),Heat affected zone (HAZ) and Fusion zone (weld metal).

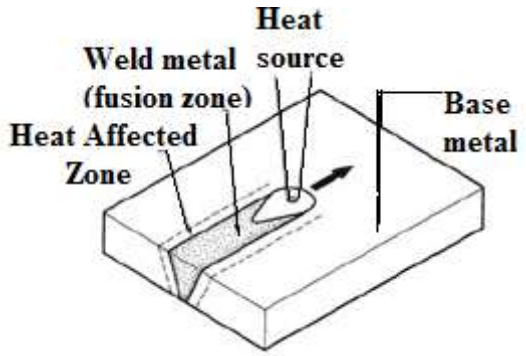

Figure 2.19 A schematic diagram showing the interaction between the heat source and the base metal in different zones [52].

Weld metal or weld zone consists of a columnar solidification microstructure similar to a cast structure [53]. Microstructures of weld metal or weld zone (fusion zone) are greatly controlled by the weld metal composition and microstructure development in weld zone also depends upon the behavior of solidification. The basic function of solidification is to control the shape and size of grains, segregation, and the inclusion, and porosity distribution. Solidification also promotes the hot cracking in weld zone [52]. For stainless steels, the differences between the parent material and weld compositions, along with the effect of dilution from the base metal into the weld pool combined with the filler materials can be understood through the Schaeffler Diagram.

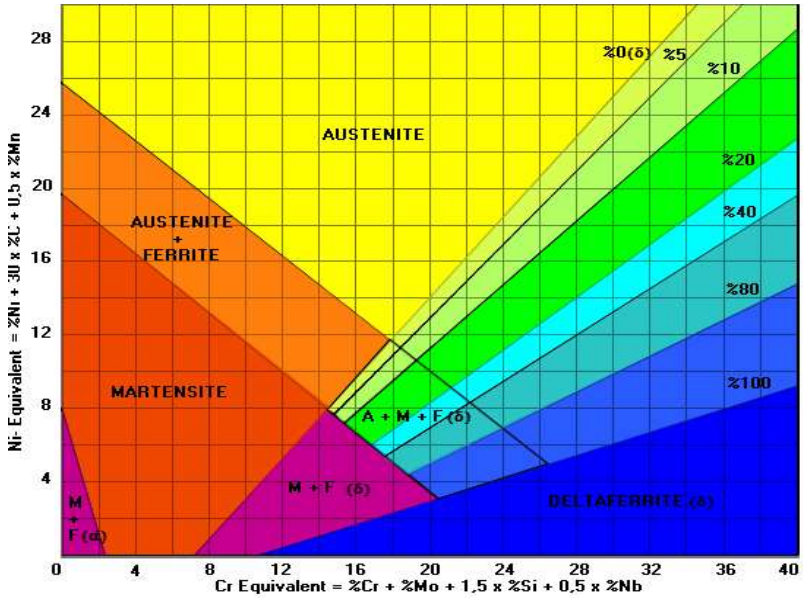

Figure 2.20 Schäffler - De Long diagram [54]

Schaeffler diagram is a powerful tool to predict the Cr-Ni austenite, austenite-ferrite or austenite-martensite weld having 0.12% of carbon. Depending on the alloying elements it contains, the Schaeffler diagram provides information on the various phases (structures) present. The Schaeffler diagram is divided into regions based on the transformation behavior of austenite. On the left side of the diagram, there is liquid to austenite and austenite to martensite transformation area, while on the right-hand side of the diagram there is liquid to ferrite transformation. In Schaeffler diagram, the austenite or ferrite, the stabilizing effect of each alloying element relative to Cr/Ni respectively, is calculated by their efficiency coefficient in the Cr or Ni equivalent formula. The original Ni_{eq} and Cr_{eq} formula used by Schaeffler is given below:

$$Ni_{eq}=\%\ Ni+30\%\ C+0.5\%\ Mn \quad \text{----------} \quad (2.3)$$

$$Cr_{eq}=\%Cr+1.8\%Mo+2.5\%Si+2\%\ Nb \quad \text{----------} \quad (2.4)$$

O. Groong and D.K Matlock, (1986) discussed the effect of welding process on the weld metal solidification structure. The shape and size of columnar grain can be changed by altered or changed the weld bead shaped [55]. Fig.2.21 through 3 schematically demonstrates the important microstructural features that must be considered during solidification in fusion welds. On a macroscopic scale, fusion welds can adopt a range of grain morphologies, in which columnar and equiaxed grains can potentially form during solidification. The final grain structure depends primarily on alloy composition and the heat-source travel speed. While the columnar and equiaxed zones can form in welds, the fine-grained chill zone at the mold wall represented by the fusion line is rarely observed in welds. Lastly, dendrite tip undercooling can become important at high solidification rates associated with highenergy- density welding processes. All of the fundamental solidification concepts i.e. nucleation, competitive grain growth, constitutional supercooling, solute redistribution, and rapid solidification depend on the solidification parameters during welding. Figure 2.21 shows the effect of travel speed on weld pool shape [56].

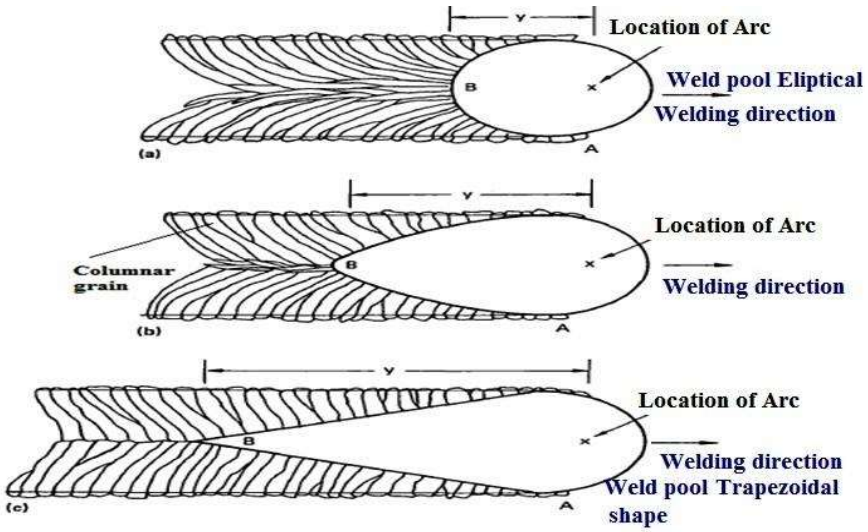

Figure 2.21 Types of grain morphologies that can form in fusion welds [57]

2.4.1.2.2 Heat affected zone (HAZ) and its properties

The region in the weldment, where peak temperature is lower than the melting temperature while high enough that the microstructure of the weldment in that region changes is known as HAZ [58]. In heat affected zone, microstructure usually depends up the following factors such as heat input, composition, peak temperature, heating and cooling rate, and electrode angle. Although it is often said that the HAZ of a weldment is its heat treated part, there is a considerable difference between welding and heat treating of, say steels [59].

The microstructure that develops in welded joints is too much influenced by the various factors such as base metal composition, filler wire used, shielding gas used, and actual cooling rate experienced by the weldment during the transformation of austenite to ferrite. The three distinct metallurgical zones that are observed is shown in figure 2.22, namely, the base metal (BM) unaffected zone, Heat affected zone (HAZ) and the fusion zone (FZ). Figure 2.22 show of different zone in a low carbon steel weldment.

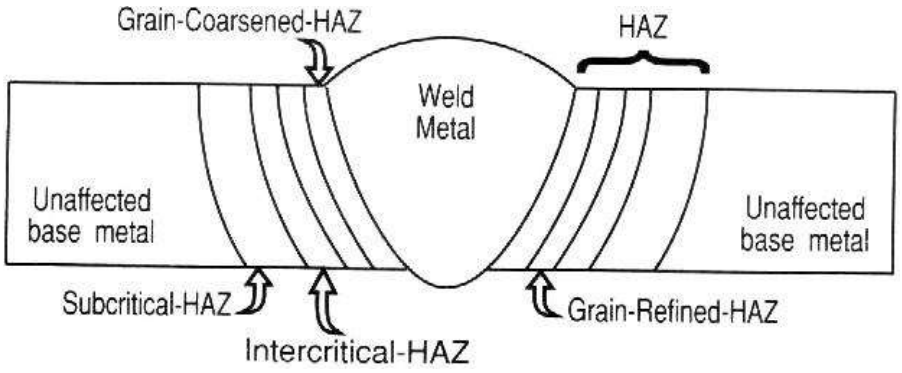

Figure 2.22 A sketch showing the three regions of a weldment (BM=base metal, HAZ=heat affected zone and FZ=fusion zone) [60]

Apurv Choubey and Vijaykumar S. Jatti, (2014) observed from the result that HAZ area adjacent to the fusion boundary was coarse-grained HAZ which possessed low hardness whereas the HAZ area adjacent to the base metal was fine-grained HAZ, which possessed high hardness. It is also observed that there is significant grain coarsening in the HAZ of all the joints. Further, it is observed from the optical micrographs that the extent of grain coarsening in the HAZ increases with increase in heat input [61].

Honggang Dong, Xiaohu Hao, Dewei Deng, (2014) showed that on increasing the heat input restrained the formation of martensite and promoted the transformation of martensite to bainite. When the welding heat input was 0.67kJ/mm, the microstructure in HAZ was fine lower bainite with some acicular ferrite. In HAZ upper bainite was produced when the welding heat input was 0.77kJ/mm, and Vickers hardness of HAZ and Fusion Zone of HSLA steel joints was much higher than that of the parent metal. The average hardness of HAZ decreased with increasing the welding heat input [62].

M. Sadeghian et al (2014), they concluded that the HAZ of the HSLA shows different transformations. Due to thermal cycles, a rapid cooling evolved, which is the case of upper bainite phase. However, the polygonal ferrite and perlite with heterogenic distribution are obtained when the cooling rate is slow [63].

Weld area can be recognized as the area that includes the weld metal and HAZ portion. The HAZ in weldment can be further divided into four main regions such as CGHAZ, fine-grained supercritical HAZ (FGHAZ), intercritical HAZ (ICHAZ) and subcritical HAZ (SCHAZ). Among

these, CGHAZ is the most affected region during welding operation due to swift cooling which caused hardening, which in turn can be the most important factor of cleavage cracking. Figure 2.23 shows the formation of coarse grain heat affected zone.

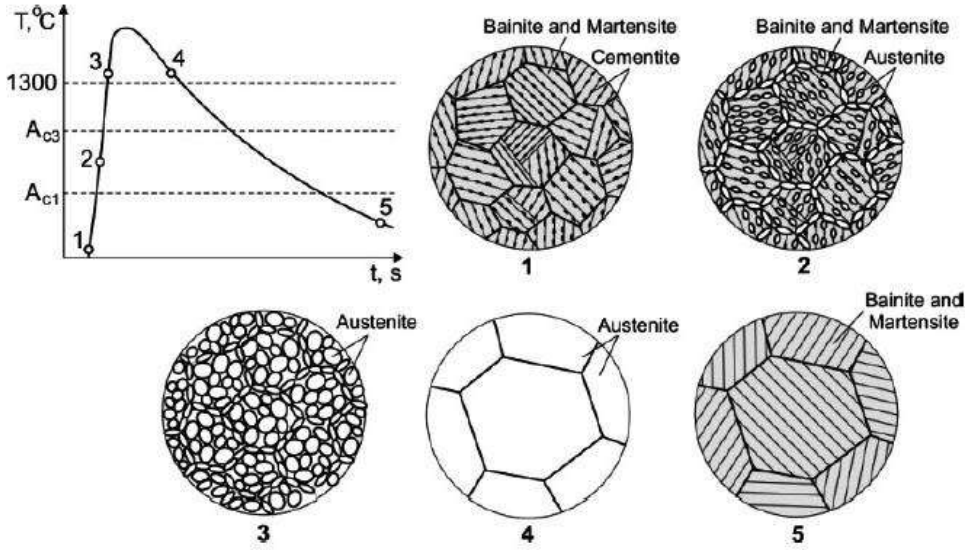

Figure 2.23 Schematic of CGHAZ formations [64]

From figure 2.24 the HAZ in steels can be sub-divided into the following zones. Starting from the weld metal side:

(i) Under Bead Zone i.e., that part of HAZ which is heated to beyond the critical temperature of Grain growth and extend up to the weld metal (fusion boundary) zone,

(ii) Grain Growth Zone, beyond 1150 °C to peritectic temperature.

(iii) Grain Refined Zone, 950 to 1150 °C, i.e., beyond A_3 up to grain refined temperature range,

(iv) Inter critical Zone, 750 to 950 °C, i.e., between A_1 and A_3 temperature.

(v) Tempered Zone of 550 to 750 °C, i.e., below A_1,

(vi) Unaffected zone (parent material) up to 550°C

Figure 2.24 shows the schematic diagram of HAZ area with different temperature range during steel welding. The width of HAZ usually depends upon the cooling rate and heat input.

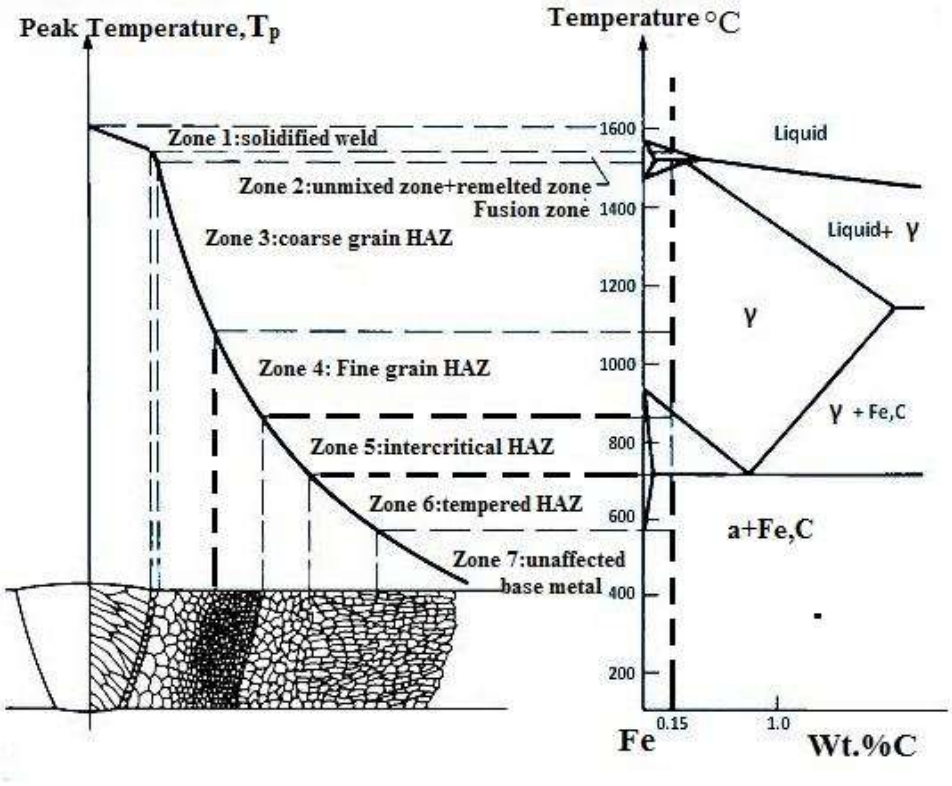

Figure 2.24 Schematic diagram of the different zone in a heat affected zone of a low carbon steel weldment [65]

In figure 2.24 each zone depicts a different type of microstructure, and perhaps more significantly, every type of structure possesses different mechanical properties. For instance, the larger austenite grain size can shift the CCT curve to longer times generating more widmanstatten ferrite, or on cooling, increasing the possibility of a product of martensite or bainite transformation.

2.4.1.3 Pre and post-weld heat processing

Preheat, as defined within the AWS Standard Welding Terms and Definition, is "the heat applied to the base metal or substrate to attain and maintain preheat temperature". The preheat temperature is defined by the same document as "the temperature of the base metal in the volume surrounding the point of welding immediately before welding is started. In the welding of a low carbon steel and alloy steel, the final microstructure of welded joint is understood by the cooling rate from the peak temperature. For instance, a procedure for welding mild steel, which has a low carbon content, relatively low hardenability, and is used in an application with no special service requirements, may consider a minimum preheat and inter-pass temperature based on the material

thickness. Welding procedures used for the heat-treatable low alloy steels and chromium-molybdenum steels with impact requirements will normally specify a minimum and maximum requirement for preheating and inter-pass temperatures. These low alloy materials can have high hardenability and are susceptible to hydrogen induced cracking.

Reasons for preheating are:

(i) To drive away moisture from the weld area

(ii) To lower the thermal gradient

(iii) To reduce the risk of hydrogen cracking

(iv) To reduce the hardness of Heat affected zone of a weldment

(v) To reduce the shrinkage stress during cooling and improve the distribution of residual stress

2.4.1.4 Post weld treatment

Post weld treatment of a weldment is performed due to following reasons:-

a) Post-weld heat treatment is mostly performed to stress relief from weldment. The purpose of stress relieving is to remove any internal or residual stresses that may be present from the welding operation.

b) For some alloy steels, a thermal tempering treatment may be necessary to obtain a suitable metallurgical structure. This treatment is generally performed after the weld has solidified.

c) Extremely coarse weld structures in steel, such as those obtained with the electro-slag welding process, may require normalizing after welding. This treatment will refine the coarse grain structure, reduce stresses after welding, and remove any hard zones in the heat-affected zone.

2.5 Microstructural Constituent in Steel weldment

On cooling the steel weldment as mentioned below, various types of microstructure are reported for low carbon steel by using the light optical microscope (LOM) I,e ferrite, pearlite, acicular ferrite (AF), bainite, polygonal ferrite(PF), grain boundary ferrite (GBF), and Widsmantatten ferrite(WF). For low carbon steel, at the temperature from 1350 $^{\circ}$C and 910 $^{\circ}$C austenite is stable and present in the primary form of microstructure which is maintained during the solidification within the temperature range. In a weldment, on solidification Grain boundary ferrite is the first phase to be generated at all temperatures and at lower temperature range the widmanstetten ferrite is formed, while on higher temperatures grain boundary allotriomorphs are produced [66]. Formation of grain boundary ferrite and widmanstatten ferrite decreases the weld toughness as they provide preferential paths for crack propagation. The α-ferrite having a BCC structure, resulting in limited solubility of carbon in iron.

2.6 Iron-Carbon Phase Diagram

An iron carbon diagram is plotted in between the carbon contents, and temperature, and used to express the different phases. Figure 2.25 depicts an iron carbon diagram. On heating, pure iron undergoes a change in its crystal structure. Carbon acts as an interstitial impurity in iron. The solubility of carbon is different at different temperature and present in the different form (Phase) of steel. In α-ferrite, the solubility of carbon in iron is 0.008% by weight at room temperature. On increasing the temperature I,e above at 723°C, the solubility of carbon increases in α-ferrite up to 0.022 % by weight. α- ferrite has a BCC structure and γ ferrite has FCC structure and solubility of carbon range goes up to 2.14 % at 1147°C temperature, which is recognized as a eutectic point. This zone is also referred as austenite, is constant in between the temperature of 723°C to 1494°C.

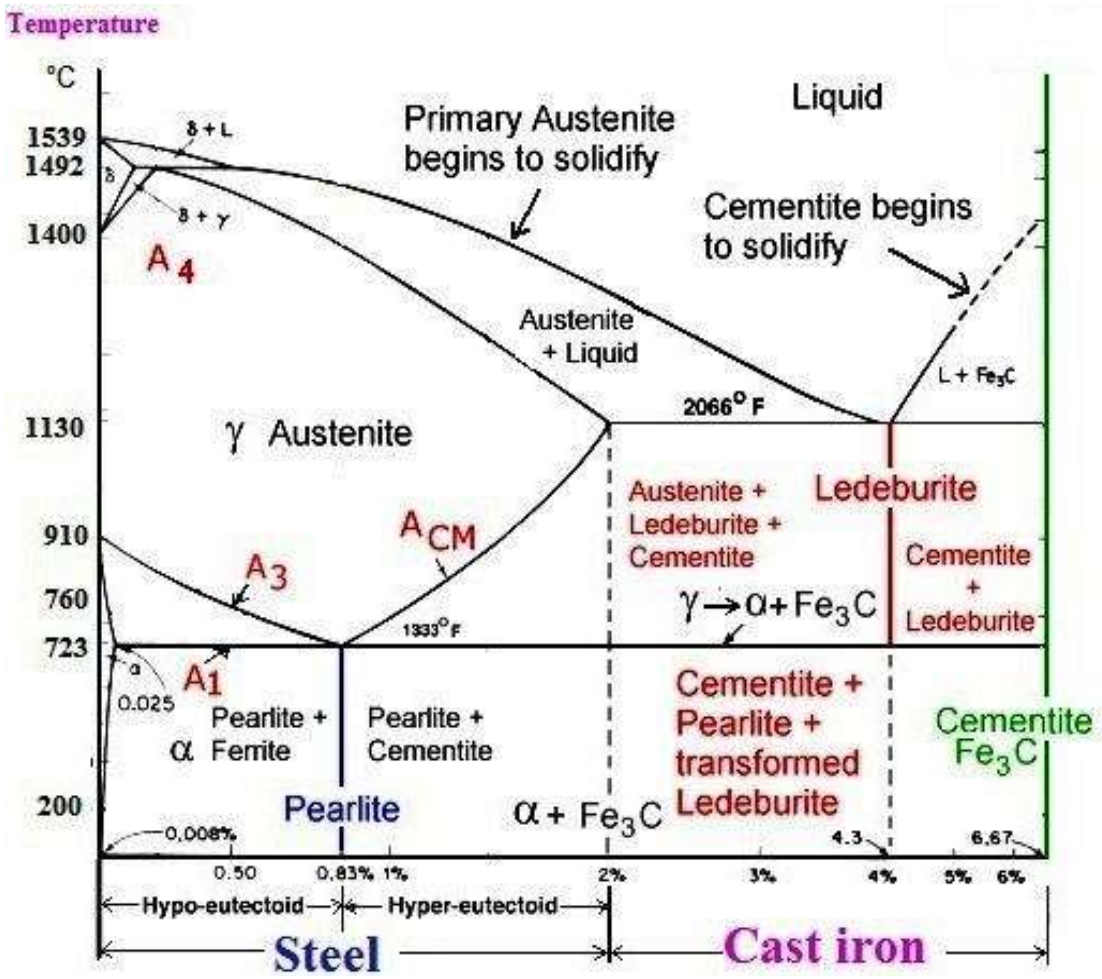

Figure 2.25 Iron-carbon phase diagram, showing the different equilibrium phases of carbon and iron with respect to varying the carbon concentration and temperature [67]

δ-ferrite which is crystallographically same to α-ferrite exists from 1394 °C up till the melting point of iron I,e 1539 °C. **δ**-iron, on cooling below at 1490 °C completely transforms into austenite and this point is referred as the peritectic point. α- iron and cementite formed when austenite cooled down from 723 °C temperature. This point is known as eutectoid point, and the boundary line is known as Ae_3 line. On increasing the carbon contents, the cementite (Fe_3C) phase is formed and this phase is very hard and brittle due to the presence of more carbon contents. Steels, a ferrite material, frequently used in a wide range of industries. On the basis of carbon contents, these alloys can be broad categories into two groups, namely, steel and cast iron. Apart from the reactions taking place in the binary Fe_3C system, on adding the alloying elements, the properties of steels change. For instance, austenite stabilizers are applied to extend the temperature range of

austenite formation and ferrite stabilizers. Some common austenite stabilizers used in steel industries are Chromium, Nickel, manganese, vanadium, molybdenum, silicon, and tungsten are ferrite formers.

2.6.1 Ferrite

Usually, three types of ferrite constituent's formation take place in a weld metal; allotriomorphic ferrite, widmanstetten ferrite, and acicular ferrite. Allotriomorphic ferrite and widmanstetten ferrite are formed at high temperature in low carbon steel. They are not observed in high strength steel weldment. Ferrite is a body-centered cubic (BCC), form of iron and it is represented by α, hence known as α iron. It is this crystalline structure which gives steel and cast iron their magnetic properties. Mild steel (carbon steel with up to about 0.2 % C) consist mostly of ferrite and increasing amounts of cementite in a laminar structure, which is called pearlite.

2.6.2 Acicular ferrite

Acicular ferrite has been known as to be most desirable microstructure consistent in steel weldment as its presence directly correlates with improved toughness, and acicular ferrite is a microstructure of ferrite in steel which is recognized by needle-shaped crystallite or grains when 2-D viewed, and it is denoted by α_a and it is formed in the same temperature range as bainite usually 400^{o}C to 600^{o}C by the same type of transformation mechanism. Oxides and non-metallic inclusion serve as nucleation sites for acicular ferrite. Acicular ferrite forms within the columnar austenite grains in competition with widmanstatten ferrite. Acicular ferrite is also recognized by high angle boundaries between ferrite grains. In 3-D, it is observed to be in the form of lenticular plates with dimensions from 5-10μm in length and 1 μm in diameter. The major classical difference between acicular ferrite and bainite is that it nucleates intragranularly in the appearance of isolated plates radiation from a point nucleation site, relatively that the cluster morphology of traditional bainite which nucleate at austenite grain boundary. In general acicular ferrite is not found in wrought steel. Figure 2.26 Schematic diagram shows different constituents of the primary microstructure in the columnar austenite grains of a steel weldment.

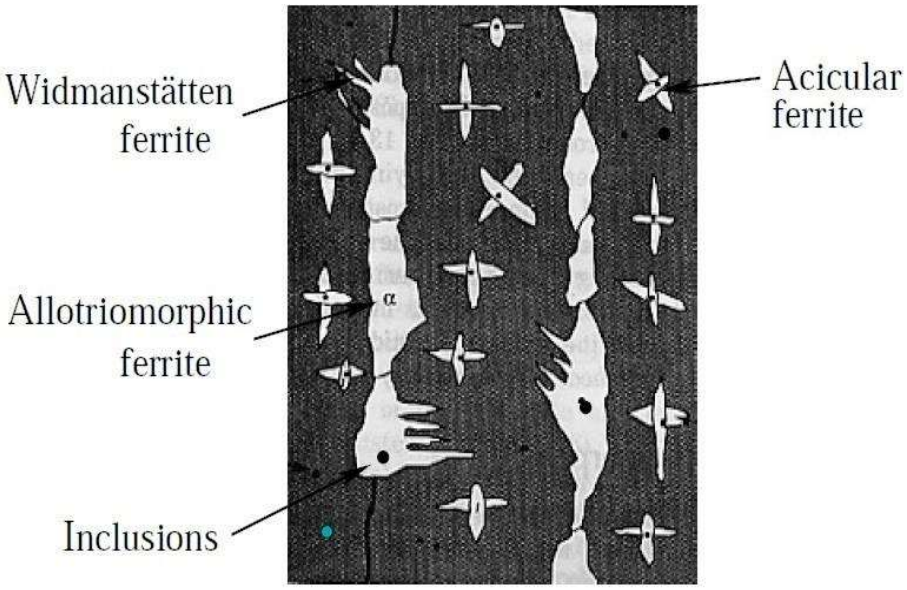

Figure 2.26 Schematic diagram showing different constituents of the primary microstructure in the columnar austenite grains of a steel weld [68]

2.6.2.1 There are some common points between acicular ferrite and bainite

- There is no substitutional solute partitioning during the growth of either acicular ferrite or bainite (Strangwood and Bhadeshia, 1987 a).
- Acicular ferrite only forms below the bainite start temperature (Ito et al 1982)
- Both reactions stop when the austenite carbon concentration reaches a value where it becomes thermodynamically impossible to achieve diffusionless growth (Yang and Bhadeshia, 1987 a, Strangwood and Bhadeshia, 1987 a).
- Like upper and lower bainite, it is possible to produce upper and lower acicular ferrite. Plates of lower acicular ferrite, like lower bainite, contain fine precipitates of cementite in a single orientation (Sugden and Bhadeshia, 1989b).
- There is a large and predictable hysteresis in the temperature at which austenite formation begins from a mixed microstructure of acicular ferrite and austenite, or bainite and austenite (Yang and Bhadeshia, 1987 b, c, 1989b).

Formation of acicular ferrite involves thermal activation. Based on this assumption; one can explain the nucleation rate/unit. Volume/Sec (I_v) can be expressed by the given expression [68]

$$I_v = \gamma \exp\{-\frac{\Delta G}{kT}\} \text{----------(2.5)}$$

Where γ is the attempt frequency, k is the Boltzmann constant; T is the temperature in Kelvin and ΔG is activation energy for nucleation/unit volume of the matrix.

2.6.3 Allotriomorphic ferrite (AF) or Grain boundary Allotriomorphs (GBA) in a weldment

Some researcher's informed that allotriomorphic ferrite (α) is first phase formation during the cooling of low carbon steel weldment at below the AC_3 temperature shown in the iron-carbon diagram in figure 2.25. It is also formed by the diffusional mechanism in two main ways: allotriomorphic and idiomorphic ferrite and the term "idiomorphic" imply that the phase concerned has faces belonging to its crystalline form. These are equiaxed crystals which nucleate inside the austenite grains, usually on non-metallic inclusion or other heterogeneous nucleation sites present in steel. The morphology of the ferrite is similar to a layer and not affects its crystal symmetry. Increasing the hardenability of the weld metal by adding some alloying elements such as Cr, Ni, V_d, and M_o, decrease the amount of allotriomorphic ferrite.

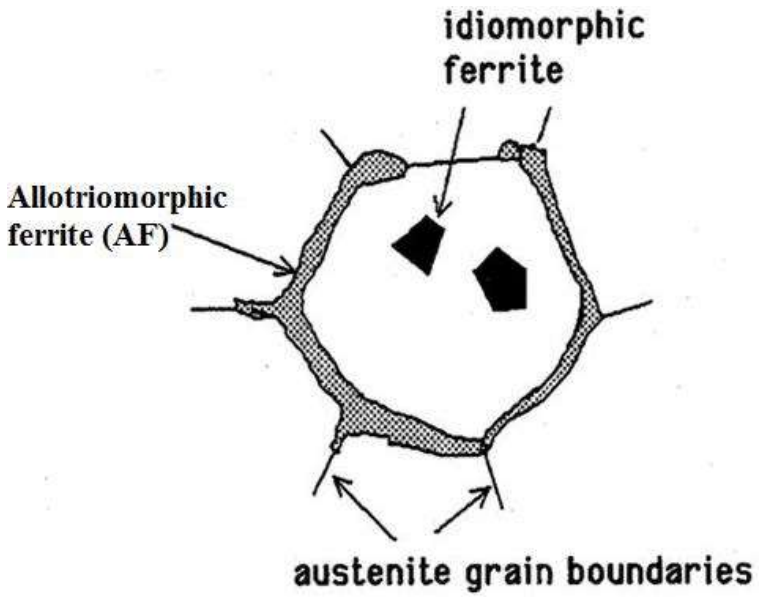

Figure 2.27 Schematic diagram of grain boundary allotriomorphic ferrite, and intragranular idiomorphic ferrite [69]

In plain carbon steels, allotriomorphic ferrite is a dominant phase over the broad range of temperature and composition. It is observed that transformation occurs with α nuclei forming a moderately coherent interface with only one adjustment austenite grain, while a random relation exists with the other. The growth of α has been shown in common a diffusion controlled process.

2.6.4 Widmanstatten ferrite

It is also known as Thomson structure. Widmanstatten ferrite is made up of long and pointed ferrite plates which involve the simulation growth of pairs of the plate. Widmanstatten classified in two categories I,e primary widmanstatten ferrite and secondary widmanstatten ferrite. Figure 2.28 shows the primary and secondary phases of widmantatten ferrite. Primary ferrite forms directly from austenite grain boundaries which are not a part of allotriomorphic ferrite whereas secondary widmanstatten ferrite forms at the allotriomorphic ferrite-austenite boundary and grows asset of parrel plates separated by the thin area of austenite. Formation of widmanstatten ferrite and grain boundary ferrite is due to the high temperature and low cooling rate at the HAZ region adjacent to the weld fusion zone [70-72]. It is also believed that during the continuous cooling, the transformation temperature of widmanstatten ferrite is just below the allotriomorphic ferrite. The widmanstatten ferrite transformation temperature is just below that of grain boundary ferrite and assumed to begin when the growth of the latter ceases. Figure 2.26 and 2.28 shows the mixture of allotriomorphic ferrite, widmanstatten ferrite, and pearlite for low carbon steel.

2.6.4.1 Following factors are responsible for the formation of widmanstatten ferrite:

- Size of austenite grain.
- Chemical composition.
- Cooling rate.
- The thickness of allotriomorphic ferrite.

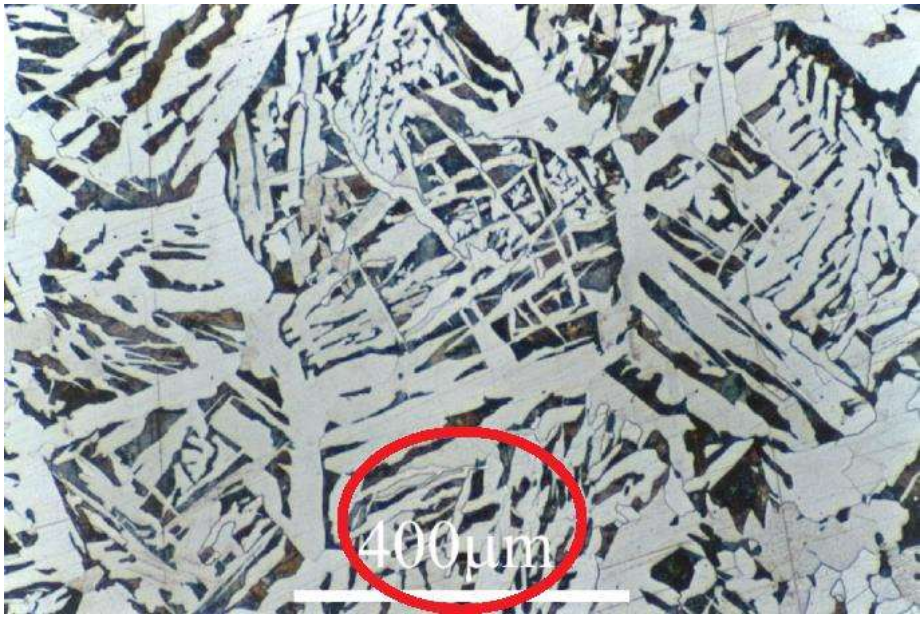

Figure 2.28 Mixture of allotriomorphic ferrite, widmanstatten ferrite, and pearlite for low carbon steel [73]

In the microstructure of low carbon steel weldment, the volume fraction (V_w) of widmanstatten ferrite can be calculated by considering the widmanstatten ferrite to nucleate at α/ γ boundaries and grow into the inner of the columnar austenite grains; the latter is again considered to be hexagonal prism and end effects are neglected.

Let us assume that α_w nucleation rate/unit area of α/ γ interface is constant; the volume fraction of widmanstatten ferrite is expressed by the following:

$$V_w = \{C_4 G (L - 4q'C_1) t_2^2 / L^2\} \text{ ---------- (2.6)}$$

Where C_4= Constant independent of alloy composition,

G=Lengthening rate of V_w

L/2=cross sectional side length of hexagonal austenite grain,

q'=corrected value of α thickness

t_2=interval of time in which α_w grows.

Formation of widmanstatten ferrite is only concern with hypoeutectic steel. It has been observed that low carbon steel having 0.3% of carbons are susceptible to the formation of widmanstatten ferrite in HAZ of weldment [74-75]. Formation of a fine structure of widmanstatten ferrite, granular ferrite improves the ultimate tensile strength of weldment. On increasing the welding current the heat input increases, which encourage the formation of widmanstatten ferrite [76-77]. Yield strength and ultimate tensile strength of steel weldment increase with an increase in the volume fraction of widmanstatten ferrite and a reduction in ferrite grain size [78]. According to International Institute of Welding (IIW), widmanstatten ferrite and its associated microphases are as ferrite with aligned martensite-austenitic-carbide (MAC) [2.73]. Widmanstatten ferrite, like the allotriomorphic ferrite, is regarded as an undesirable constituent it leads to poor fracture toughness [79-80].The average length and thickness of widmanstatten ferrite α_w in Fe-Ni-Si-C steel was measured, and the mean value was recorded to be 156 μx and 1.4 μm respectively, after considering sectioning effects [81].

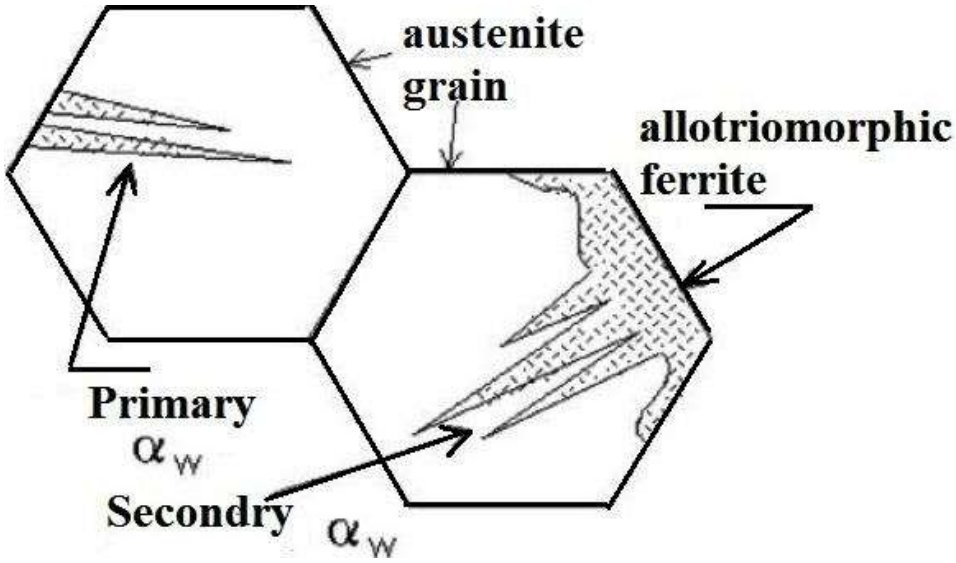

Figure 2.29 shows the primary and secondary phases of widmanstatten ferrite [81]

2.6.5 Pearlite

The lamellar structure of pearlite results from the diffusion and co-operative development of cementite and ferrite within austenite cooled just under the lower critical temperature. This is identified as eutectoid reaction and reaction can be expressed as:

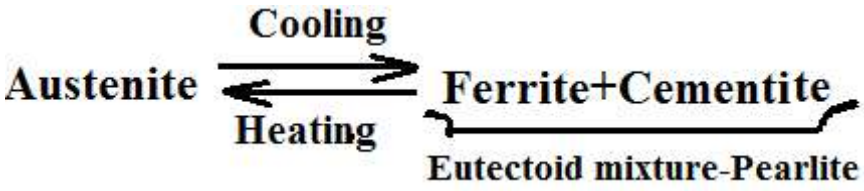

The pearlite formation in steel consists co-operative, the diffusional growth of cementite and ferrite from austenite. As discussed earlier, pearlite is an alternative layer of cementite and ferrite and it is also well explained in an iron carbon diagram. The main constituents in pearlite are 88% ferrite and 12% cementite. Another important characteristic to point out is that the ferrite produced here has a very little carbon content, which makes it approximately pure iron whilst the other phase is cementite. Carbon from the austenite grain boundary then diffuses into this platelet. It enhances the size of the cementite platelet. Figure 2.30 shows the actual microstructure of IS 2062 steel weldment having ferrite and pearlite.

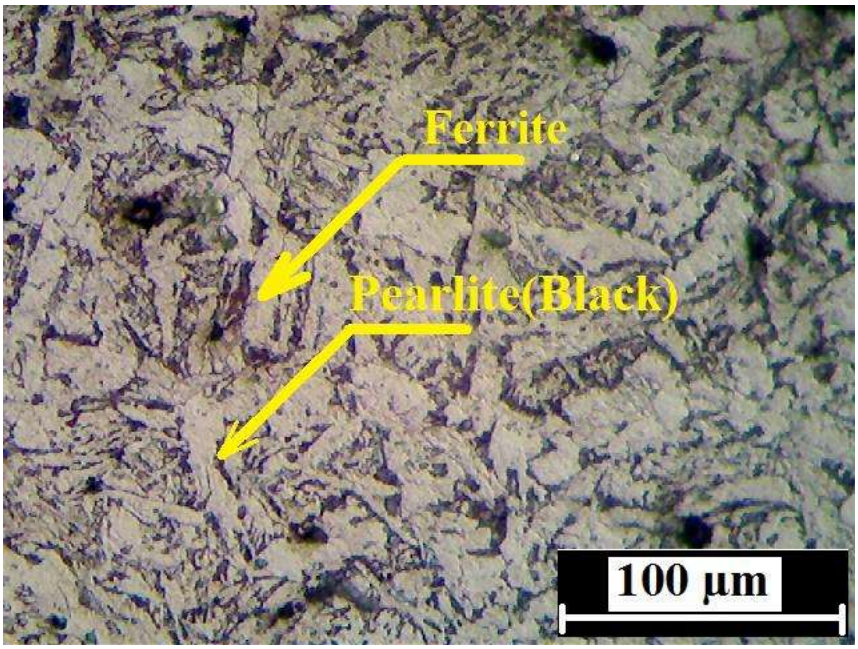

Figure 2.30 shows the ferrite (White) and Pearlite (Black) in the low carbon steel weldment

2.6.6 Austenite

Austenite is a face-centered cubic (FCC) structure. In iron carbon diagram, it is stable at the temperature above 723^{o}C, depending upon the carbon content present. It can dissolve carbon up to 2% by weight.

2.6.7 Bainite

Bainite was discovered in the early 1930's by Bain and Davenport [2.76]. Ferrite and carbide mixture is referred as bainite, and bainite formation takes place over a wide range of temperature. Bainitic microstructure which produced in welding process of steel may influence the weldment hardness and weldment strength. It is important to understand and control the transformation to bainite and its effect on mechanical quality of a weldment. Bainite is a non-lamellar aggregate of the plate formed of carbide and ferrite. Sometimes bainite forms as a part of a mixed microstructure of a weldment consisting pearlite, widmanstatten ferrite, acicular ferrite, martensite. Due to the fine structure of bainite, it can be only studied with an electron microscope. Figure 2.31 shows the morphological classification systems for bainite as per Bramfitt and Speer. The key features of the different classes of bainite are given as follows:

- B_1 incorporates an intralath constituent that may be cementite or ε-carbide.
- B_2 is composed of interlath particle or film, which can be cementite, austenite or martensite.
- B_3 incorporates discrete regions of retained parent phase or secondary transformation product.

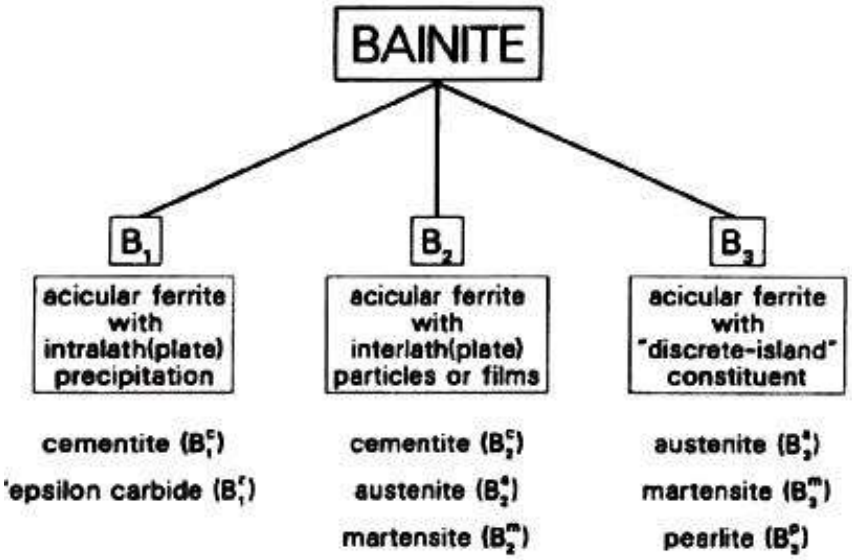

Figure 2.31 Morphological classification systems for bainite according to Bramfitt and Speer [82]

There are two types of bainite, upper bainite produced at high temperature and lower bainite produced at lower temperature [68]. Both bainites are distinguished by their shape, size and their lath size. Dendrite core regions of the low carbon weld metals a mixture of upper bainite, lower bainite formed. The big difference between classical bainite and acicular ferrite is the fact that it nucleates intragranularly in the form of isolated plates radiating from a point nucleation site. Figure 2.32 shows the schematic representation of the transition from upper and lower bainite. In bainite, size of ferrite plate is 10μmx0.2μm.

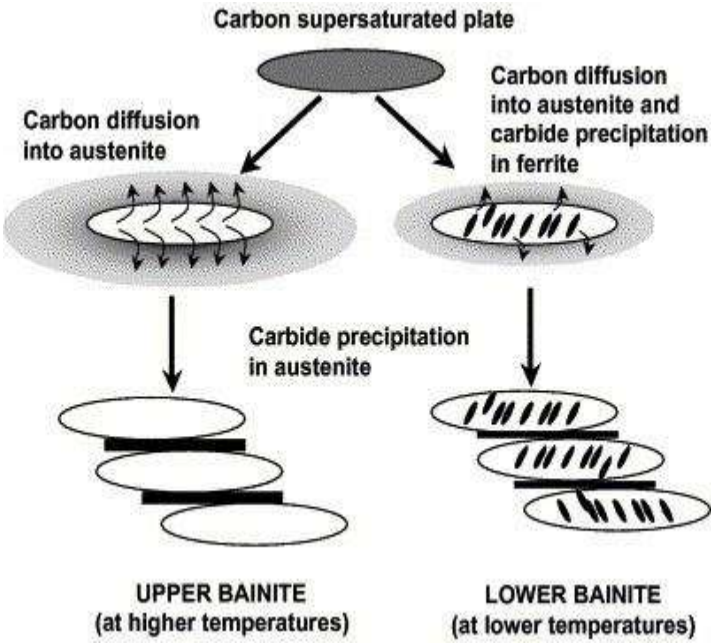

Figure 2.32 Schematic representation of the transition path of upper and lower bainite [68]

2.6.7.1 Upper bainite

Upper bainite consists of the plate of ferrite near to each other, which are very nearly the same crystallographic orientation in space. Upper bainite is formed at around 400-550 $^{\circ}$C in sheaves (growth of plates take place in clusters called as sheaves).

2.6.7.2 Lower bainite

Lower bainite is quite similar to upper bainite, except that the amount of interplate cementite is low, and carbide can be found within the ferrite plate itself. Lower bainite formed at 250-450 ^{o}C. This intra-ferrite carbide can be epsilon carbide in the case of high carbon steel or cementite in case of low carbon steels. It has been calculated that epsilon carbide will not be generated in bainitic ferrite for steels with a carbon content lower than 0.55% by wt. in lower bainite, there are interplate carbide and intra-ferrite carbides.

2.6.8 Martensite

Martensite is very hard and less ductile. It is a product of diffusionless transformation and its formation may be in the form of thin, lenticular plates. At rapid cooling rates, the austenite may

reach the temperature of 400^{o}C or below it, depending on alloying, before transformation. Transformation at these temperatures is a diffusionless process to the formation of lath martensite.In α-iron martensite is considered as a supersaturated solution of carbon. Figure 2.33 shows the structure of martensite, cementite, and ferrite in carbon steel. Martensite has a body-centered tetragonal (BCT) structure.

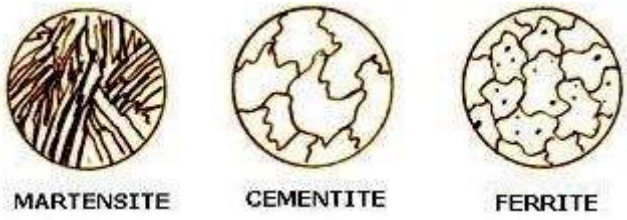

Figure 2.33 shows the structure of martensite, cementite, and ferrite in a microstructure [83]

When martensite is heated up to a temperature of 600 $^{\circ}$C, it became to start to soften and toughness of steel improved. Figure 2.34 a shows two unit cells of austenite (grey circles) with carbon at their octahedral interstices (black circles). It is expressed in the figure 2.34 that these two unit cells are bonded at their (100) $_{F}$ planes to embrace the BCT structure on martensite (Fig 2.34 b and Fig 2.34 c).In order to describe the transformation of the austenite (FCC) lattice into the martensite (BCT/BCC) lattice, Bain proposed a concept dealing with the structural change realized by a homogeneous deformation [84].

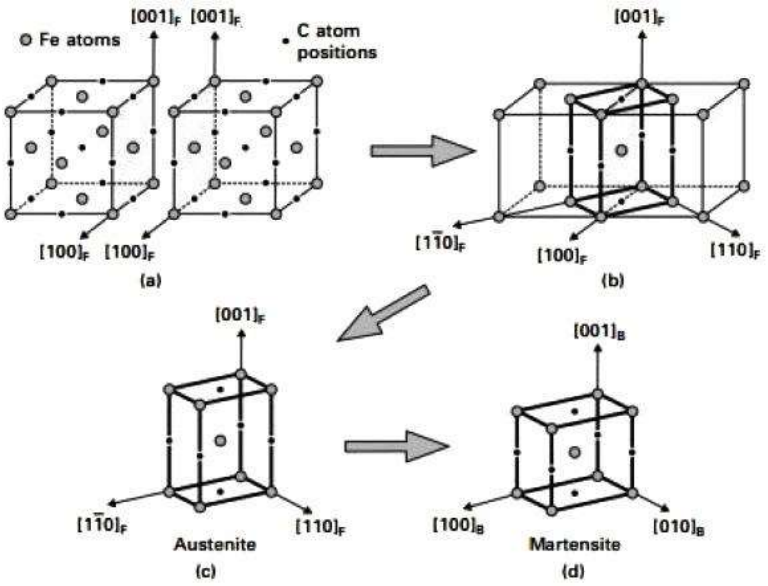

Figure 2.34 The Bain model for martensite formation in steels [84]

Figure 2.35 shows a time-temperature curve for steel, to the formation of the different constituent such as ferrite, pearlite, bainite, widmanstatten ferrite and martensite at different temperature range.

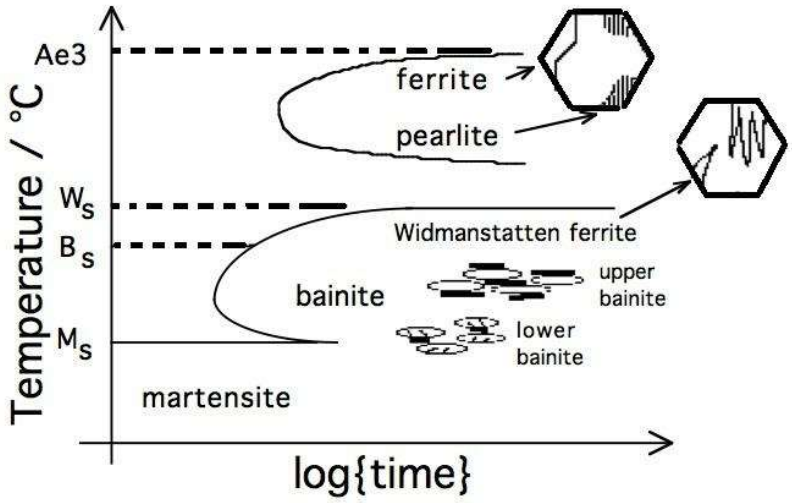

Figure 2.35 shows the formation of martensite, bainite etc. [73]

2.7 Characteristics of IS 2062 steel and AISI 304 steel

Steel is perhaps the most "advanced" material of world. It is a versatile metallic material with a wide range of superior mechanical properties, from moderate yield strength range (200-300MPa) with excellent ductility, which can be produced at a very nominal production cost. It has a vast range of applications. Steel is not new innovation which leads to a general misperception that everything is known about steel, amongst those outside its field. In general, steel is defined as ferrous alloys containing less than 2%C by weight [85]. One of the unique properties of steel is the high strength-to-weight ratio, and corrosion resistance and its alloys amongst the most versatile engineering, petrochemical, food process and pharmaceutical industries in recent year [6].

2.7.1 IS 2062 steel

IS 2062 steel or mild steel (iron-containing a small percentage of carbon, tough and strong but not readily tempered), also referred as plain-carbon steel and low-carbon steel, is now the most

common form of steel as its cost is comparatively low while it provides material properties that are adequate for numerous applications. Mild steel consists approximately 0.05–0.25% carbon making the IS 2062 steel ductile and malleable. On increasing the more carbon contents, the steel is classified as cast iron. Mild steel has a fairly low tensile strength, but it is inexpensive and simple to form; surface hardness can be improved through carburizing process. IS 2062 or mild steel is not an alloy steel and hence do not have large amounts of other elements. Since its carbon and alloying elements content are comparatively low, there are several properties it has that distinguish it from high carbon and alloy steels. Weldability, machinability, and castability of IS2062 or mild steel are relatively excellent that makes it such a popular for consumers. IS 2062 or mild steel also having a high amount iron and ferrite, making it magnetic.

2.7.1.1 Common Applications of IS 2062 steel

Here are some examples of where it is used in the world:

- Structural steel
- Signs
- Automobiles
- Furniture
- Decorations
- Wire
- Fencing
- Nails

2.7.2 Stainless steel

Stainless steels usually contain chromium between 10-20% as the major alloying element and are valued for high corrosion resistance. Therefore it is known as corrosion resistant steel. Due to the presence of 11% chromium, steel is about 200 times more resistant to corrosion as compared to IS 2062 steel or mild steel. On the basis of their crystalline structure, stainless steels can be divided into five major groups:

2.7.2.1 Austenitic steel

Austenitic steels are non-magnetic and non-heat-treatable and generally consisting 18% chromium, 8% nickel, and approximate 0.8% less than carbon. Austenitic steels acquire the largest portion of the global stainless steel market and are often used in food processing industries, kitchen utensils, petrochemical, and piping industries. Corrosion resistance properties of this type of steel can be improved by adding chromium, molybdenum, and nitrogen.

2.7.2.2 Ferritic steel

Ferritic steels consists trace amounts of nickel, 12-17% chromium, less than 0.1% carbon, along with other alloying elements, such as molybdenum, aluminum or titanium. These magnetic steels cannot be hardened by heat treatment process but their strength can be improved by the cold working process. Ferritic steel is not formable as austenitic stainless steel.

2.7.2.3 Martensitic steel

Martensitic steels having 11-17% chromium, less than 0.4% nickel, and carbon up to 1.2%. These magnetic and heat-treatable steels are used in the fabrication of knives, cutting tools, as well as dental and surgical types of equipment as they have high strength and moderate corrosion resistance properties. They possess low weldability and formability.

2.7.2.4 Duplex steel

These steels having a microstructure consisting approximate 50% ferritic and 50% austenitic, this provides then a greater strength as compared to ferritic, and austenitic steels. The unique feathers of duplex steel that they are resistant to stress corrosion cracking. They consist moderate formability, and they are magnetic but not as much as the ferritic, martensitic, and precipitation hardening steel only due to 50% austenitic phase.

2.7.2.5 Precipitation hardening steel

Precipitation hardening stainless steels are chromium and nickel containing steels which provide a most favorable combination of the properties of martensitic and austenitic grade steels. Like martensitic grades, they are recognized for their ability to gain high strength through heat treatment and they also have the corrosion resistance of austenitic stainless steels.

The high tensile strengths of precipitation hardening stainless steels achieved after a heat treatment process that leads to precipitation hardening of a martensitic or austenitic matrix. Hardening is done by addition of one or more of the elements such as copper, aluminum, titanium, niobium, and molybdenum.

2.7.3 Common Industrial applications of AISI 304

In this research work AISI 304 chosen as workpiece material because AISI 304 having the following advantages.

Some common applications of AISI 304 are listed below:-

- Culinary uses
  - Kitchen sinks
  - Cutlery
  - Cookware
- Surgical tools and medical equipment
  - Hemostats
  - Surgical implants
  - Temporary crowns (dentistry)
  - Orthopedic implants (Predominantly 316 / 316L)
  - Artificial heart valves (Predominantly 316 / 316L)
  - Bone fixation
  - Mandrels / tools
  - Medical needles
- Architecture (pictured above: Chrysler Building)
  - Bridges
  - Monuments and sculptures
  - Airport roofs
- Automotive and aerospace applications
  - Auto bodies
  - Rail cars

- Aircraft

- Medical Applications
  - Orthopedic implants (Predominantly 316 / 316L)
  - Artificial heart valves (Predominantly 316 / 316L)
  - Bone fixation
  - Mandrels / tools
  - Chemical containers / Hazardous waste containers
  - Wires
  - Wire Coils
  - Wire forms
  - Specialty guide wires
  - Curettes
  - Screws / prostheses / plates
  - Medical syringes

- Domestic – cutlery, sinks, washing machine drums, microwave oven liners, razor blades etc.

- Architectural/Civil Engineering – cladding, handrails, door and window fittings, street furniture, structural sections, reinforcement bar, lighting columns, lintels, masonry supports

- Transport industries – ship containers, ships chemical tankers etc.

- Chemical industries –pressure vessels, process piping. Oil and Gas – platform accommodation etc.

- Medical – Surgical instruments, surgical implants, MRI scanners etc.

- Food and beverage industries – Catering equipment, brewing, distilling, food processing.

- General purpose industries– springs, fasteners (bolts, nuts, and washers), wire etc.

2.7.4 Classification of steels

Classification of steels on the basis of structure and on the basis of the commercial name of steels is shown in figure 2.36

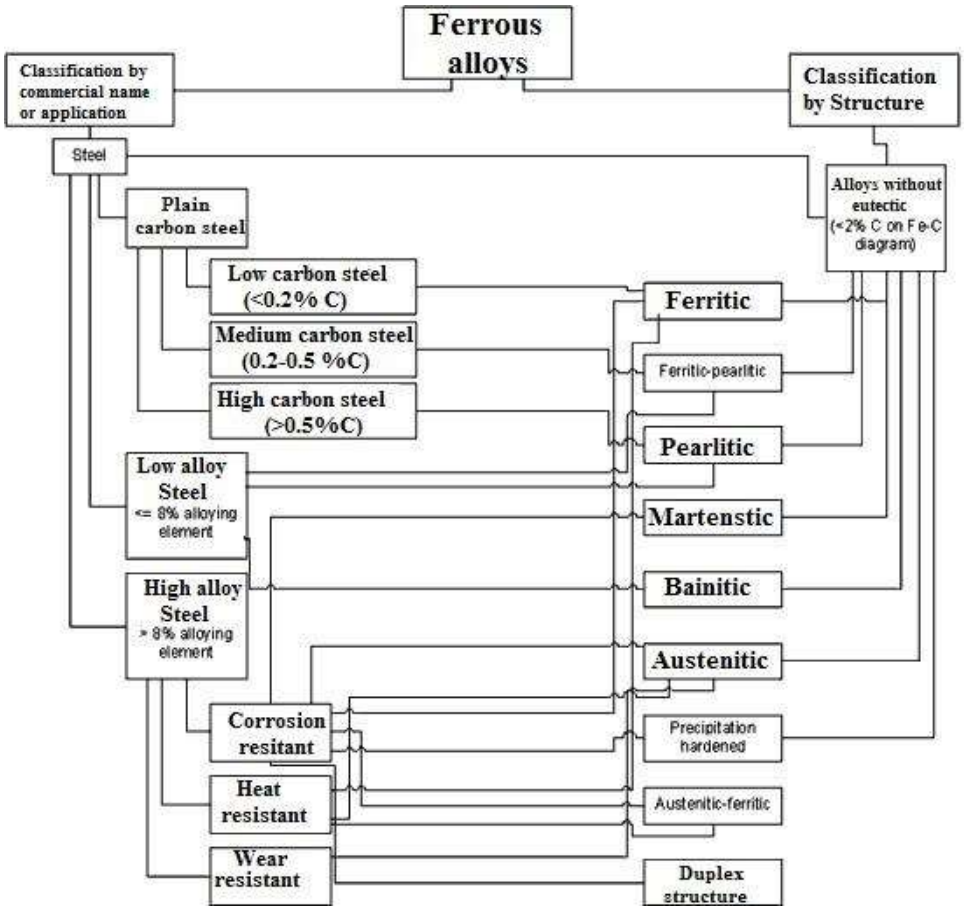

Figure 2.36 classifications of Steels [85]

2.7.5 Differences between IS2062 steel and AISI 304 steel:

Some common differences between mild steel and AISI 304 steel are given below

- AISI 304 is known as 18/8 steel. Whereas IS 2062 steel is known as structural steel.
- In AISI 304 due to presence chromium, it is corrosion resistant steel, whereas there is very little presence of chromium in IS 2062 hence IS 2062 is not corrosion resistant steel.

- In microstructure of IS 2062, there is a 75% of ferrite and 25% of pearlite is the presence, while in the microstructure of AISI 304, there is the presence of δ-ferrite with austenite matrix in skeleton form.
- IS 2062 contains carbon as their main constituent, while AISI 304 contains chromium as an alloy.
- In IS 2062 carbon lies between 0.05-0.25 percent, whereas in AISI 304 chromium lies min.10% by wt.
- For IS 2062 to prevent corrosion a galvanizing layer is required, whereas in AISI 304 no layer is required as it naturally averse to corrosion.
- The tensile strength of IS2062 steel depends upon the carbon component, whereas AISI 304 is a high tensile strength material.
- IS 2062 steel having low hardness, while AISI 304 having the high level of hardness.
- IS 2062 steel is magnetic while Stainless steel may or may not be magnetic.
- Cost of IS 2062 steel is very low comparatively AISI 304 steel.
- IS 2062 steel is used for the structural purpose, whereas AISI 304 steel is used for food, process, pharmaceutical, nuclear industries.

2.8 Solidification mechanism of Steel weldment

Microstructural examination during solidification of the fusion zone represents one of the most significant considerations for controlling the weldments properties. A wide range of microstructural features forms in the weld zone (fusion zone), depending on the composition of alloys, welding parameters, and solidification rate. In solidification, grain structure depends mainly on alloy composition, heat-source, and travel speed. Solidification controls grain structure, microstructure, porosity, inclusion distribution, hot-cracking behavior, and, ultimately, weld-metal properties.

Important parameters, in solidification mechanics, that influence microstructure are listed below:

Temperature gradient G, growth rate (R), undercooking (ΔT), and alloy composition (Co). The effect of the growth rate R and the temperature gradient G on the solidification microstructure of alloys is expressed in Figure 2.37. Together, R and G control the solidification microstructure. The ratio G/R evaluates the mode of solidification while the products GR control the size of the solidification structure.

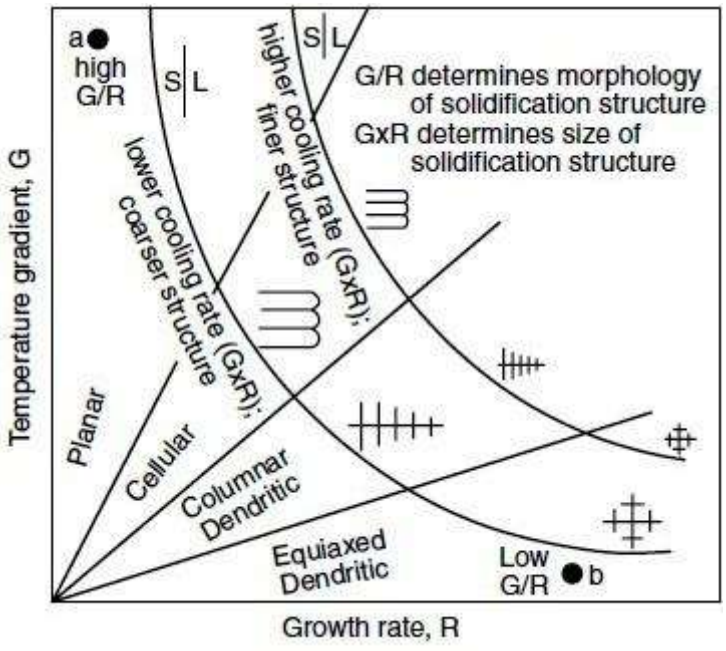

Figure 2.37 Effect of temperature gradient G and growth rate R on the morphology and size of solidification microstructure [67].

The grain structure is considerable additionally complex in fusion welding process, as the pool shape forms a curved solid/liquid interface that is frequently in motion because it follows the heat source this is expressed in figure 2.38 [67]. Grains for growth, formed at the fusion mine in a constructive direction, but their direction may become unfavorable as the curved solid/liquid boundary changes its location. These grains may then in due course be overgrown by other grains that exhibit additionally favorable orientation for growth as the solid/liquid boundary sweeps via the weld.

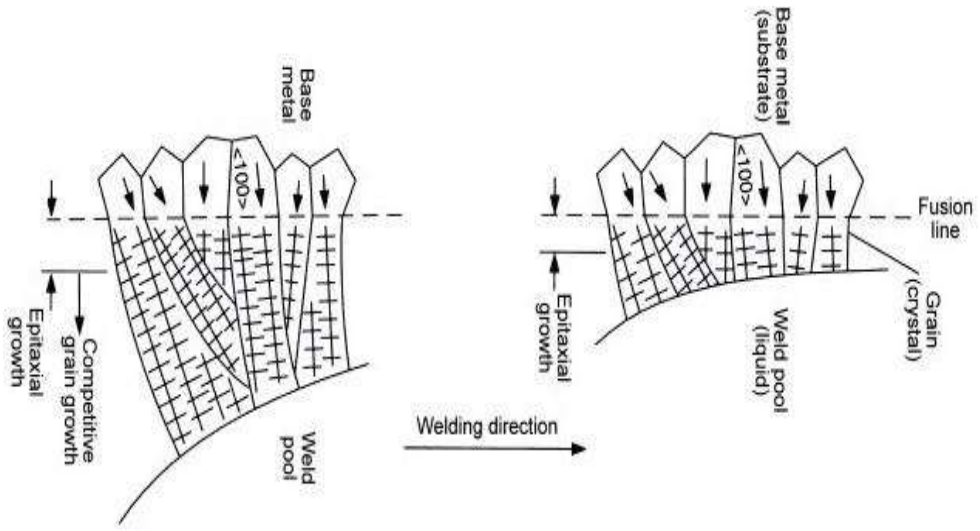

Figure 2.38 Schematic illustrations of competitive grain growth in welds. (a) Early growth of grains near the fusion line. (b) Continued growth of favorably orientated grains at a later time [67].

Solidification morphologies as well, as the formation mechanism of lacy ferrite and vermicular found in the austenitic stainless steels, solidified with primary ferrite (FA mode) was clarified in terms of crystallography. The growth manner of the primary ferrite and secondary austenite is termed as “independent two-phase growth”. The ferrite morphology is determined by both the crystallographic orientation relationship between ferrite and austenite established at the step of nucleation of ferrite and the relationship between the welding heat source direction and the preferential growth directions of austenite and ferrite [86].

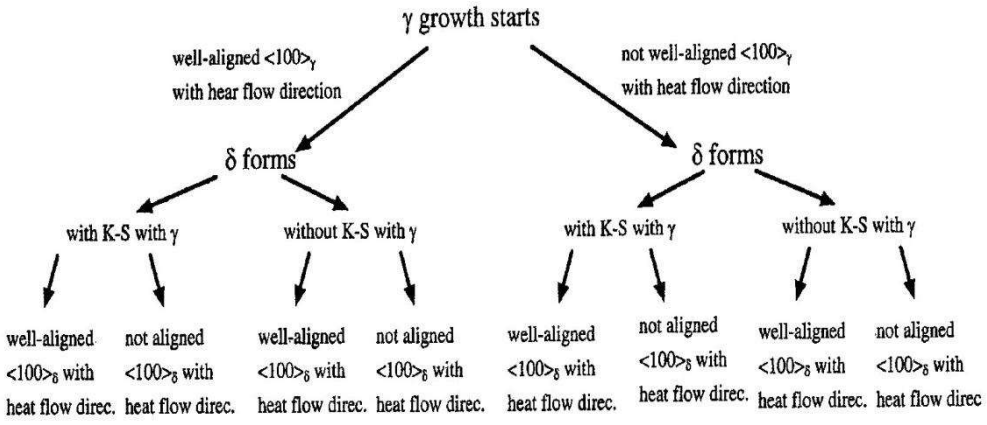

Case	A	B	C	D	E	F	G	H
Initial morph.	Lacy	Lacy	Vermicular	Vermicular	Lacy	Lacy	Vermicular	Vermicular
δ status	continues	dies off, replaced by new δ	continues	dies off, replaced by new δ	continues	dies off, replaced by new δ	continues	dies off, replaced by new δ
γ status	continues	continues	continues	continues	dies off, replaced by aligned γ	dies off, replaced by aligned γ	dies off, replaced by aligned γ	dies off, replaced by aligned γ
Final morph	Lacy	Vermicular (Case C) or Lacy (Case A)	Vermicular	Vermicular (Case C) or Lacy (Case A)	Vermicular	Vermicular (Case E or G)	Vermicular	Vermicular (Case E or G)

Figure 2.39 Proposed mechanisms for the formation of different ferrite morphologies in weld metals solidified in FA mode [86]

SA David et al (1996), developed a model to prediction of welded joint microstructure development, as a function of weld metal composition and welding process parameters, for any alloy system and they informed that for low alloys steel, the nucleation and growth of oxide inclusion in the melt was considered as a function of welding process. The microstructure is depended on cooling rate and solidification modes.

The dendrites or cells in the weld metal are not always discernible.

A number of continuous-cooling transformation (CCT) curves have been plotted schematically to describe the development of the weld metal microstructure of low-carbon steel, and low-alloy steels. The one expressed in Figure 2.39 is based on that of Onsoien et al. The hexagons stand for

the transverse cross-sections of columnar austenite grains in the weldment. Since austenite (III) is cooled down from high temperature, ferrite (IV) nucleates at the grain boundary and grows inward. The grain boundary ferrite (GBF) is also referred "allotriomorphic" ferrite, meaning that it is a ferrite having a no regular faceted shape reflecting its inner crystalline structure. At lower temperatures the mobility of the planar growth front of the Widmanstatten ferrite and grain boundary ferrite (GBF) reduces, also referred side-plate ferrite, forms instead. These side plates can extend quicker because carbon, instead of piling up at the planar growth front, is pushed to the sides of the growing tips. Substitutional atoms do not spread while the growth of Widmanstatten ferrite. At even lower temperatures it is very slow for Widmanstatten ferrite, to produce to the grain interior and it is faster if new ferrite nucleates ahead of the growing ferrite. This new ferrite, that is acicular ferrite, nucleates at inclusion particles and has arbitrarily oriented tiny ferrite needles with a basket weave feature.

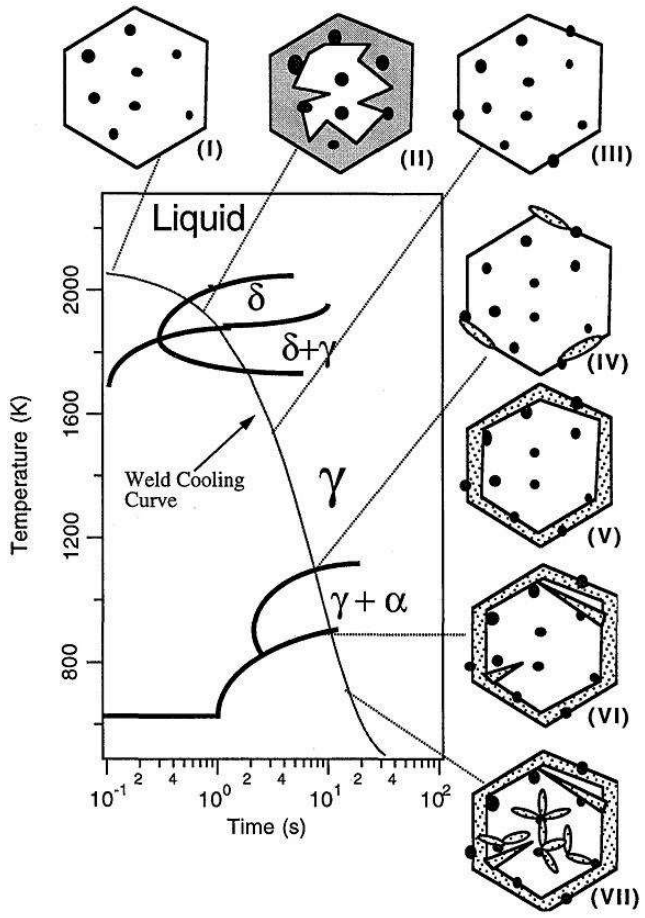

Figure 2.40 Schematic diagram of continuous cooling transformation depict the development of weldment microstructure in low-alloy steel:- (I) inclusion formation,(II) solidification of liquid to δ- ferrite,(III) fully austenitic structure,(IV) nucleation of allotriomorphic ferrite,(V) growth of allotriomorphic ferrite all along the austenite grain boundaries,(VI) widmanstatten ferrite formation, and (VII) acicular ferrite formation [87]

2.9 Summary

1. The effect of different welding parameters on mechanical properties and microstructure of IS 2062 structural steel and AISI 304 steel has been studied. The variation in mechanical properties have been try to correlate with microstructure of weldment.
2. In this report the experimental investigation have been carried out to determine the effect of different welding parameters under different conditions. 300 mm x120 mm x10 mm and 260 mm × 70 mm × 5 mm workpiece cut out from IS 2062 and AISI 304 steels. Two machined (V-groove) workpiece is clamped in a fixture, on the welding table. Motion of welding table is control with the help of control panel.IS 2062 steel workpiece were welded at 25-28V, 7.62-11.43 m/min, and 10-25 l/m for AISI 304 steel T 20-23V, 6.35-10.16 m/min, and 10-25 l/m .
3. Mostly researchers worked on a single material with a constant wire feed speed and constant shielding gas flow rate or tried to weld two different materials. Further work is essential to understand the effect of GMA welding parameters on mechanical properties and microstructure of weld zone (WZ) and heat affected zone (HAZ) and understanding the fracture mode.
4. The mechanical properties i.e. yield strength, ultimate tensile strength, toughness, Vickers hardness, and percentage of elongation of IS 2062 and AISI 304 steel weldment were determined. The variations in yield strength, ultimate tensile strength, and percentage elongation and microhardness at different heat input have been shown graphically.

2.10 Research gap

Mostly, work has been done by the researcher on the single material to determine the effect of different welding parameters on mechanical properties and microstructure of i.e. IS 2062 or AISI 304 steel. Therefore, the research of two individual workpiece i.e. IS 2062 and AISI 304 were

selected to determine the effect of GMA welding parameters at 25-28V at 7.62-11.43 m/min wire feed speed, 10-25 l/m shielding gas flow rate, and 3.22 to 4.47 kJ/mm heat input for IS 2062 structural steel and 20-23V at 6.35-10.16 m/min wire feed speed, 10-25 l/m shielding gas flow, and 1.89 to 3.01 kJ/mm heat input for AISI 304 steel.

Mechanical properties and microstructure of IS 2062 steel and AISI 304 steel weldment were compared with the previous research work under different welding conditions and it was observed that our results were matching with the previous researchers work and it was also observed that on increasing the heat input ,adversely affect the mechanical properties.